RESEARCH MEMORANDUM

LOW-SPEED CHARACTERISTICS OF A 45° SWEPTBACK WING OF ASPECT RATIO 8 FROM PRESSURE DISTRIBUTIONS AND FORCE TESTS AT REYNOLDS NUMBERS FROM 1,500,000 TO 4,800,000

By Robert R. Graham

Langley Aeronautical Laboratory
Langley Field, Va.

NATIONAL ADVISORY COMMITTEE
FOR AERONAUTICS

WASHINGTON
October 22, 1951

NACA RM L51H13 ~~RESTRICTED~~

NATIONAL ADVISORY COMMITTEE FOR AERONAUTICS

RESEARCH MEMORANDUM

LOW-SPEED CHARACTERISTICS OF A 45° SWEPTBACK WING OF ASPECT RATIO 8 FROM PRESSURE DISTRIBUTIONS AND FORCE TESTS AT REYNOLDS NUMBERS FROM 1,500,000 TO 4,800,000

By Robert R. Graham

SUMMARY

Results are presented of an investigation in the Langley 19-foot pressure tunnel of the longitudinal characteristics of a wing having 45° sweepback of the quarter-chord line, an aspect ratio of 8, a taper ratio of 0.45, and NACA 63_1A012 airfoil sections parallel to the plane of symmetry. The results were obtained from force measurements through a Reynolds number range from 1,500,000 to 4,800,000 and pressure-distribution measurements at Reynolds numbers of 1,500,000 and 4,000,000. The effects of fences and leading-edge roughness on the characteristics of the wing were investigated by means of force and pressure-distribution measurements at a Reynolds number of 4,000,000.

The results of the investigation indicated that the wing pitching-moment variations were caused by section-lift variations on the outboard portions of the wing and not by section pitching-moment variations. The wing pitching-moment curve changed from a stable slope at zero lift to an unstable slope at fairly low lift coefficients and became progressively more unstable as maximum lift was approached. The changes in pitching-moment-curve slope were due to separation on the outboard section which first caused a reduction in section-lift-curve slope and finally caused a loss in section lift. The section pitching-moment variations became more stable as the wing maximum lift was approached.

Varying the Reynolds number from 1,500,000 to 4,000,000 caused the outboard separation and hence the wing pitching-moment instability to be delayed to slightly higher lift coefficients. At Reynolds number of 4,000,000, fences delayed the outboard separation to much higher angles of attack, with the result that the wing pitching-moment curve was linear almost to maximum lift. The pitching-moment variation was

still unstable at the stall, however. Adding leading-edge roughness to the wing at a Reynolds number of 4,000,000 caused the section lift and wing pitching-moment variations to be somewhat similar to those at the low Reynolds number.

The maximum lift-coefficient of the wing was about 1.01 and was not affected by changes in Reynolds number or by leading-edge roughness. Reducing the Reynolds number or adding leading-edge roughness, however, increased the angle of attack at which maximum lift was attained. The fences increased maximum lift coefficient to 1.07.

Varying the Reynolds number, adding leading-edge roughness, or installing fences on the wing had practically no effect on the root section-lift curves which were almost linear to the highest angle of attack of the tests (31°).

INTRODUCTION

Sweptback wings have been the subject of much experimental and theoretical research in the past few years since their advantages for high-speed flight became apparent. Most of the research, however, has been limited to the low-aspect-ratio range. Increasing interest in long-range, high-speed airplanes has created a demand for information on swept wings in the higher aspect-ratio range.

Accordingly, the low-speed characteristics of a wing of aspect ratio 8 with the quarter-chord line swept back 45° were investigated in the Langley 19-foot pressure tunnel. The wing was untwisted and had a taper ratio of 0.45 and NACA 63_1A012 airfoil sections parallel to the plane of symmetry. The investigation included the determination of the characteristics of the wing by force and pressure-distribution measurements.

The tests were made at a Reynolds number of 4,000,000 and a Mach number of 0.19. The effects of varying the Reynolds number from 1,500,000 to 4,800,000 and of leading-edge roughness were investigated. The effects of one configuration of chordwise fences were also investigated.

SYMBOLS

The data are referred to the wind axes with the origin at projection on the plane of symmetry of the quarter chord of the mean aerodynamic

chord. The data have been reduced to nondimensional coefficients which are defined as follows:

C_L lift coefficient $\left(\frac{L}{qS_w} \text{ or } \int_0^1 c_l \frac{c}{\bar{c}} d\left(\frac{y}{b/2}\right)\right)$

c_l section lift coefficient

$$\left(\cos \alpha \int_0^1 \left(S_u - S_l\right) d\left(\frac{x}{c}\right) - \sin \alpha \int_{-(z/c)_{max}}^{(z/c)_{max}} \left(S_r - S_f\right) d\left(\frac{z}{c}\right)\right)$$

c_{l_b} section lift coefficient at zero wing lift due to model and stream misalinement

C_D drag coefficient $\left(\frac{D}{qS_w} \text{ or } \int_0^1 c_d \frac{c}{\bar{c}} d\left(\frac{y}{b/2}\right)\right)$

c_d section pressure drag coefficient

$$\left(\sin \alpha \int_0^1 \left(S_u - S_l\right) d\left(\frac{x}{c}\right) + \cos \alpha \int_{-(z/c)_{max}}^{(z/c)_{max}} \left(S_r - S_f\right) d\left(\frac{z}{c}\right)\right)$$

C_m pitching-moment coefficient

$$\left(\frac{M}{qS_w c'} \text{ or } \int_0^1 \left(c_m - \frac{x_{c/4}}{c} \int_0^1 \left(S_u - S_l\right) d\left(\frac{x}{c}\right)\right) \frac{c^2}{\bar{c}c'} d\left(\frac{y}{b/2}\right)\right)$$

c_m section pitching-moment coefficient about local quarter chord

$$\left(\int_0^1 \left(S_u - S_l\right)\left(0.25 - \frac{x}{c}\right) d\left(\frac{x}{c}\right) + \int_{-(z/c)_{max}}^{(z/c)_{max}} \left(S_r - S_f\right) \frac{z}{c} d\left(\frac{z}{c}\right)\right)$$

C_b bending-moment coefficient about root chord line

$$\left(\int_0^1 \frac{c}{\bar{c}} \frac{y}{b/2}\left(\int_0^1 (S_u - S_l)\, d\left(\frac{x}{c}\right)\right) d\left(\frac{y}{b/2}\right)\right)$$

$C_{\tau_{c/4}}$ twisting-moment coefficient about swept quarter-chord line

$$\left(\int_0^1 c_m \frac{c^2}{\bar{c}c'}\, d\left(\frac{y}{b/2}\right)\right)$$

$C_{\tau_{c_{r/4}}}$ twisting-moment coefficient about lateral axis through quarter chord of root

$$\left(C_{\tau_{c/4}} - \frac{\bar{x} - x_{c_{r/4}}}{c'}\int_0^1 \frac{c}{\bar{c}}\left(\int_0^1 (S_u - S_l)\, d\left(\frac{x}{c}\right)\right) d\left(\frac{y}{b/2}\right)\right)$$

R Reynolds number $\left(\frac{\rho V c'}{\mu}\right)$

M_o stream Mach number

α angle of attack, degrees

α_b section angle of attack at zero wing angle of attack due to model and stream misalinement

L lift

D drag

M pitching moment about 0.25c'

S_w wing area

c' mean aerodynamic chord $\left(\frac{2}{S_w}\int_0^{b/2} c^2 dy\right)$

c local wing chord parallel to plane of symmetry

$\bar{c}$ mean chord $\left(\frac{S_w}{b}\right)$

c_r	root chord
b	wing span
q	dynamic pressure $\left(\frac{1}{2}\rho V^2\right)$
V	free-stream velocity
μ	coefficient of viscosity
ρ	density of air
S	pressure coefficient $\left(\frac{H - p}{q}\right)$
H	free-stream total pressure
p	local static pressure
x	longitudinal distance from local leading edge measured parallel to chord plane and plane of symmetry (rearward positive)
$x_{c/4}$	longitudinal distance from quarter chord of c' to local quarter chord (rearward positive)
$x_{c_r/4}$	longitudinal distance from quarter chord of c' to quarter chord of root
x'	longitudinal distance from local quarter chord to local center of pressure
$\bar{x}$	longitudinal distance from quarter chord of c' to centroid of normal force (chordwise center of pressure)
y	lateral distance from plane of symmetry measured perpendicular to plane of symmetry
$\bar{y}$	lateral distance from plane of symmetry to centroid of normal force (spanwise center of pressure)
z	vertical distance from chord plane measured perpendicular to chord plane (up, positive)
$\bar{z}$	vertical distance from chord plane to centroid of chordwise force (vertical center of pressure)

if $P = \frac{p - p_o}{q}$ where p_o = freestream static,

$P = 1 - S$

Subscripts:

u	upper surface
l	lower surface
f	forward of maximum thickness
r	rearward of maximum thickness

MODEL AND APPARATUS

The general dimensions of the model used in the investigation are shown in figure 1. The model was made of steel covered with a thin layer of an alloy of bismuth and tin. It had an aspect ratio of 8.02, a taper ratio of 0.45, and 45° sweepback of the quarter-chord line. The airfoil section parallel to the plane of symmetry was the NACA 63_1A012, and its ordinates are given in reference 1. The wing was untwisted.

The model was equipped with surface orifices for measuring the pressure distribution on the left-hand panel over the full chord at seven spanwise stations and around the leading edge at a station at 0.03b/2 as shown in figure 1. Pressures over the rearward portion of the airfoil at the 0.03b/2 station were read by means of a static pressure tube located about 0.0035c from the wing surface. The tubes connected to the orifices were brought out of the model from the lower surface of the right-hand panel at a point about 20 percent of the semispan out from the plane of symmetry. From that point the tubes were conducted back through a pipe fixed to the wing and parallel to the chord plane and then down through a fairing through the floor of the tunnel to multitube manometers. The pressures on the manometers were simultaneously recorded by means of cameras. The tube conducting pipe was replaced by a flush cover plate for the force tests. The model is shown installed in the tunnel for the force tests in figure 2 and for the pressure-distribution tests in figure 3.

For some of the tests, fences were installed as shown in figure 4. The fences were $\frac{1}{16}$-inch sheet steel fastened to the wing parallel to the plane of symmetry with angle clips. For tests with roughness, 0.011-inch-diameter carborundum grains were spread over a surface length of 8 percent of the chord back from the leading edge on the upper and lower surfaces along the full span of the wing. The grains were thinly spread to cover from 5 to 10 percent of that area and were held in place by a thin coat of shellac.

TESTS

The model was tested in the Langley 19-foot pressure tunnel with the air compressed to about $2\frac{1}{3}$ atmospheres. The Reynolds numbers and their corresponding Mach numbers obtained in the investigation are as follows:

R	M_o
1.5×10^6	0.07
2.2	.11
3.0	.14
4.0	.19
4.8	.25

Lift, drag, and pitching moment were measured at those values of Reynolds and Mach numbers through an angle-of-attack range extending beyond maximum lift. In addition, pressure-distribution measurements were made at 1,500,000 and 4,000,000.

CORRECTIONS TO DATA

The data obtained from force tests have been corrected for the tare and interference effects of the model supports. The angle of attack and drag and pitching-moment coefficients obtained from force tests and pressure-distribution tests have been corrected for jet-boundary effects by adding the following increments as determined from reference 2:

$$\Delta\alpha = 0.39C_L$$

$$\Delta C_D = 0.0063C_L^2$$

$$\Delta C_m = 0.0035C_L$$

Span loadings determined from pressure-distribution measurements indicated a basic loading at zero lift that tunnel surveys indicated was due mainly to air-stream angle variations in the region occupied by the model.

The chordwise variation of the angle of flow was averaged at several spanwise locations by representing the variation as an effective camber line. The average angle was then determined from the angle of attack of the zero lift line of the effective camber line. The zero lift lines were obtained by a method given by Munk in reference 3. The spanwise variation of the averaged stream angles from the flow measurements is presented in figure 5. The basic loading due to the spanwise angle variation is presented in figure 5 and was obtained by multiplying the angles by the slopes of the section-lift curves obtained from the pressure measurements. The basic loading obtained from pressure measurements at zero lift is also presented in figure 5. The small differences between the two basic loading curves are probably due to slight inaccuracies in the construction of the model and experimental inaccuracies in measuring the air-stream angles and model pressure distribution.

No satisfactory method is known for correcting the individual pressure coefficients (table I and fig. 6) for the basic loading, but the force and moment coefficients integrated from the pressure-distribution data have been corrected at all angles of attack by subtracting the loading obtained at zero lift. The pitching-moment coefficients from the force tests have been corrected for the moment due to the basic loading on the swept wing. The basic loading from the pressure measurements was used for correcting the data because possible model inaccuracies on the untwisted, uncambered wing would be corrected for along with the angle variation.

No correction was applied to take into account the spanwise variation of the jet-boundary-induced angle or the model twist due to loading. Calculations of the spanwise variation of the induced angles and measurements of model twist angles indicated them to be small (0.2° at $C_L = 1.0$) and of the same order of magnitude but opposite in direction.

RESULTS AND DISCUSSION

Presentation of Data

The results of the pressure-distribution tests made on the plain wing at a Reynolds number of 4,000,000 are presented as pressure coefficients in table I and figure 6. The section-lift characteristics integrated from the pressure data of table I and figure 6 are presented in figure 7. Also presented in figure 7 are the section-lift characteristics integrated from pressure-distribution data for the plain wing at a Reynolds number of 1,500,000 and for the wing with fences and with leading-edge roughness at a Reynolds number of 4,000,000.

The results of force tests on the plain wing through a Reynolds number range from 1,500,000 to 4,800,000 are presented in figure 8. The results of spanwise integrations of the section characteristics are also presented in figure 8. A few of the chordwise pressure diagrams obtained on the wing at a Reynolds number of 1,500,000 are presented in figure 9. The effects of fences and leading-edge roughness on the force characteristics of the wing at a Reynolds number of 4,000,000 are presented in figure 10.

The pressure-distribution data for the plain wing at a Reynolds number of 4,000,000 have been integrated to give section pitching-moment and drag coefficients (fig. 11), span-loading coefficients (fig. 12), spanwise, chordwise, and vertical centers of pressure (fig. 13), local chordwise centers of pressure (fig. 14), and wing bending- and twisting-moment coefficients (fig. 15).

Lift and Pitching-Moment Characteristics

The section-lift curves for the plain wing at a Reynolds number of 4,000,000 (fig. 7) show that the lift for the root sections increases nearly linearly with angle of attack up to the highest angle of the tests (31°). The lift curves for the tip sections show a decrease in lift-curve slope at low angles of attack (about 5° for the 0.96b/2 station) and a levelling off at around 10° to 12°. The combination of the linear variation at the root and the nonlinear variation at the tip causes a nonlinear pitching-moment variation for the wing. (See fig. 8.) The decreasing lift-curve slope at the tip sections causes a forward movement of the aerodynamic center which begins at about 5° angle of attack and about 0.3 lift coefficient and continues to maximum lift.

The section pitching-moment characteristics (fig. 11) have a negligible effect on the wing pitching-moment characteristics as demonstrated by the fact that at maximum lift the variations of the section pitching moments are stable while those of the wing pitching moments are unstable.

The decreasing lift-curve slope over the outboard sections is also reflected in the wing lift curve (fig. 8) where the slope starts decreasing at about 5° angle of attack. At about 20°, the increasing lift at the root is just offset by decreasing lift over the outer portions of the wing so that above an angle of attack of 20° the lift coefficient is constant at about 1.01 up to the highest angle of the tests (31°).

Effects of Reynolds number variation.- The effects of a reduction in Reynolds number from 4,000,000 to 1,500,000 on the section lift

characteristics are shown in figure 7. These effects are confined mainly to the outer semispan of the wing. The initial loss of lift is more severe at the lower Reynolds number. Following the initial loss of lift, an increase in lift occurs which results in higher lift coefficients than were obtained at the same angles of attack at the higher Reynolds number. As the angle of attack is increased further, the lift decreases again. Examination of the chordwise pressure diagrams for the lower Reynolds number (fig. 9) reveals that the first loss of lift ($\alpha = 12.9^\circ$) was caused by trailing-edge separation. The increase in lift following the initial loss of lift ($\alpha = 14.9^\circ$) occurred when separation was complete over the full chord of the 0.90b/2 and 0.96b/2 stations. At that angle of attack the loss of lift over the nose of the sections was more than offset by an increase in lift over the rearward portions. At the 0.75b/2 station the pressure diagram for $\alpha = 14.9^\circ$ shows a widening out of the low pressure area over the forward part of the section which more than offsets the loss of the peak at the leading edge. Although this diagram is similar to those obtained in the vortex type of flow (see reference 4), there was no evidence of that type of flow on this wing as shown by surveys with a single tuft of yarn on a long probe. The 0.75b/2 station was obviously in a transition region between separated and unseparated flow where the separated-flow region extended farther inboard at the leading edge than at the trailing edge. At 15.9° angle of attack the stalled region moved inboard slightly so that the low pressure region was broader and the section lift coefficient was still higher. These lift variations over the tip sections caused the pitching-moment curve for the complete wing (fig. 8) to have a decided jog just below maximum lift. At a Reynolds number of 4,000,000, these outboard lift phenomena were much less noticeable so that the pitching-moment curve showed a smaller rearward movement of the aerodynamic center at about 16° angle of attack. The lift characteristics of the root sections were unaffected by the change in Reynolds number. The maximum lift of the wing was unaffected by changes in Reynolds number in the range investigated (fig. 8), but the angle of attack at which maximum lift was first attained was reduced by increasing the Reynolds number.

Effects of fences.- The initial trailing-edge separation over the outboard sections was attributed to a thickened boundary layer due to spanwise flow along the long panel of the high-aspect-ratio wing. Blocking the spanwise flow by means of fences at the locations shown in figure 4 allowed the tip sections to reach considerably higher lift coefficients (fig. 7) before separation occurred. The root section lift characteristics were unaffected by the fences.

The delay of tip separation brought about by the fences increased the maximum lift coefficient to 1.07 and allowed the wing pitching-moment curve (fig. 10) to be almost linear to maximum lift. The

pitching-moment break at maximum lift, however, was unstable because of outboard stalling.

Effects of leading-edge roughness.- Tests at a Reynolds number of 4,000,000 with leading-edge roughness added to the wing showed that roughness caused the tip sections to have a lower lift-curve slope (fig. 7), an earlier separation, and a lower maximum lift. The tip sections with leading-edge roughness experienced the same type of increased lift after the initial reduction as was noted on the smooth wing in tests at a Reynolds number of 1,500,000. The lift characteristics of the root sections were unaffected by the leading-edge roughness. These changes in the lift characteristics of the outboard wing sections caused a slight reduction in wing lift-curve slope (fig. 10), a forward shift in aerodynamic center at zero lift, and a jog in the pitching-moment curve below maximum lift similar to that noted for the smooth wing at a Reynolds number of 1,500,000. The maximum lift coefficient for the wing was not changed by roughness, but the angle of attack at which maximum lift was attained was considerably increased.

Root section lift characteristics.- It is of interest to note that factors such as leading-edge roughness or variation in Reynolds number, which had a considerable effect on the lift characteristics of the tip sections, had no effect on the lift characteristics of the root sections in the angle-of-attack range of the tests. The stall resistance of the root sections of sweptback wings has been encountered previously (reference 5) when unsuccessful attempts were made to hasten stalling at the root to improve the pitching-moment characteristics at maximum lift. This resistance to stalling is due in part to the absence of high pressure peaks over the nose of those sections (fig. 6) and to the spanwise flow which draws low-energy air from the boundary layer of the rearward portions of those sections.

The lack of high peak pressures over the nose of the root sections is associated with the curvature of constant pressure lines across the center section as has been shown in previous pressure-distribution investigations on sweptback wings (references 6 and 7).

Drag Characteristics

The drag coefficients determined from pressure-distribution data do not include drag forces due to shearing stresses in the boundary layer of the wing. Any comparison between the force test drag and pressure drag must, therefore, be made with that in mind.

The section drag curves (fig. 11) indicate that the trailing-edge separation over the tip sections at low lift coefficients (about 0.3)

did not cause any appreciable drag increase. The drag of these sections did not start increasing very rapidly until after a wing lift coefficient of about 0.6 had been reached. At the root, however, where practically no separation occurred, the drag increases fairly rapidly from a wing lift coefficient of about 0.2. The chordwise pressure diagrams (fig. 6) show that the tip sections have the peak pressure far forward in that lift range so that the suction pressures over the nose of those sections tend to counteract the drag due to separation. The root sections, however, have much smaller peak pressures which are farther back from the leading edge than they are at the tip. The forward chordwise force is therefore very small at that station, and the drag component of the normal force is the main contributing factor in the section drag.

The fences caused an increase of about 75 percent in the drag at zero lift. (See fig. 10.) This increment could probably be reduced, however, by fastening the fences to the wing with flush clips instead of on the surface of the wing. The drag in the lift-coefficient range between 0.8 and 1.0 was reduced considerably because of the delay of separation on the outer panel.

Leading-edge roughness caused about as much increase in drag at zero lift (fig. 10) as the fences caused. In the lift-coefficient range above 0.6, the drag was increased considerably because separation over the outer panel was hastened by the roughness.

Loading Characteristics

The spanwise loading curves (fig. 12) and the spanwise center-of-pressure curves (fig. 13) show the effects of the loss of lift at the tips. The loadings at the higher angles of attack dropped off over the outer portions of the wing and were still increasing over the inboard portions at the highest angles of attack of the tests (31°). The drag loading curves show that the drag loading coefficient is greatest at the root at all angles of attack in spite of the separation on the outer panels and absence of separation over the root. The spanwise center of pressure (fig. 13) was about constant at $0.458b/2$ over the low angle-of-attack range from 0° to about 5° and then started moving inboard as the angle of attack was increased further.

The chordwise center of pressure (fig. 13) was at about $0.34c'$ at 0° angle of attack and moved forward slightly between 0° and 5°. Above 5° the center of pressure moved forward more rapidly as the angle of attack was increased, until at 21° it was at the leading edge of the mean aerodynamic chord. At 31° it had moved back to about $0.04c'$. The chordwise center of pressure is influenced more by the span-load

distribution on the swept-wing panels than by the local centers of pressure, as will be noted when a comparison of figures 13 and 14 is made. As the angle of attack is increased, the local centers of pressure all across the span move rearward (fig. 14) while the wing center of pressure (fig. 13) moves forward with increasing angle of attack.

The bending-moment coefficients (fig. 15) increase with angle of attack in a manner similar to that of the lift. The bending moment, however, tends to level off at a lower angle of attack than the lift because as the lift levels off the center of pressure moves inboard.

The twisting-moment coefficients (fig. 15) about the root of the swept quarter-chord line were practically zero up to about 12° angle of attack. This moment is a function of the section pitching moments which cause a nose-up twisting moment near the tips (fig. 11) and zero at the root because of the counteracting nose-down pitching moments of the root sections. Above 12° the slopes of the section pitching-moment curves are all in the same direction and thus produce nose-down twisting moments.

The twisting moments about a lateral axis through the quarter chord of the root (fig. 15) have much larger negative values because of the rearward location of the center of pressure of the wing lift with respect to the moment axis. The slope of the twisting-moment curve decreases as angle of attack is increased because of a decreasing lift-curve slope and a forward movement of the center of pressure.

SUMMARY OF RESULTS

The results of a low-speed investigation involving force and pressure-distribution measurements on a 45° sweptback wing of aspect ratio 8 may be summarized as follows.

Chordwise pressure diagrams and section-lift curves showed that the initial separation occurred at low angles of attack along the trailing edge of the outboard sections of the wing. The main results of the separation were a decrease in slope of the outboard section-lift curves and an unstable change in slope of the wing pitching-moment curve. Increasing the Reynolds number from 1,500,000 to 4,000,000 delayed complete separation of the outboard sections to a slightly higher angle of attack, but unstable changes in pitching moment were still evident at fairly low angles of attack because of trailing-edge separation. At a Reynolds number of 4,000,000, fences delayed the separation so that the outboard section-lift curves were nearly linear to considerably higher angles of attack, and the wing pitching-moment

curve was linear almost to maximum lift. The initial stall, however, still occurred on the outboard portions of the wing causing unstable pitching-moment variations at maximum lift. Adding leading-edge roughness to the wing at a Reynolds number of 4,000,000 caused the section lift and wing pitching-moment curves in the upper lift range to be similar to those at the low Reynolds number but also caused a reduced lift-curve slope for the outboard sections and an unstable change in slope of the wing pitching-moment curve through zero lift.

The section pitching-moment characteristics of the wing had very little influence on the wing pitching-moment characteristics. The section pitching moments had stable variations at the stall, while the wing pitching moments had unstable variations.

The maximum lift coefficient of the wing was about 1.01 and was not affected by changes in Reynolds number or by leading-edge roughness. Reducing the Reynolds number or adding leading-edge roughness, however, increased the angle of attack at which maximum lift was attained. The fences increased maximum lift coefficient to 1.07.

Varying the Reynolds number, adding leading-edge roughness, or installing fences had practically no effect on the root section-lift curves which were almost linear to the highest angle of attack of the tests (31°).

Langley Aeronautical Laboratory
National Advisory Committee for Aeronautics
Langley Field, Va.

REFERENCES

1. Loftin, Laurence K., Jr.: Theoretical and Experimental Data for a Number of NACA 6A-Series Airfoil Sections. NACA Rep. 903, 1948. (Formerly NACA TN 1368.)

2. Sivells, James C., and Salmi, Rachel M.: Jet-Boundary Corrections for Complete and Semispan Swept Wings in Closed Circular Wind Tunnels. NACA TN 2454, 1951.

3. Munk, Max M.: The Determination of the Angles of Attack of Zero Lift and of Zero Moment, Based on Munk's Integrals. NACA TN 122, 1923.

4. Lange, Roy H., Whittle, Edward F., Jr., and Fink, Marvin P.: Investigation at Large Scale of the Pressure Distribution and Flow Phenomena over a Wing with the Leading Edge Swept Back 47.5° Having Circular-Arc Airfoil Sections and Equipped with Drooped-Nose and Plain Flaps. NACA RM L9G15, 1949.

5. Graham, Robert R., and Conner, D. William: Investigation of High-Lift and Stall-Control Devices on an NACA 64-Series 42° Sweptback Wing with and without Fuselage. NACA RM L7G09, 1947.

6. Weber, J.: Low Speed Measurements of the Pressure Distributions and Overall Forces on Wings of Small Aspect Ratio and 53° Sweepback. TN No. Aero 2017, British R.A.E., Sept. 1949.

7. Weber, J., and Bredner, G. G.: Low Speed Tests on 45° Sweptback Wings. Part I. Pressure Measurements on Wings of Aspect Ratio 5. Rep. No. Aero 2374, British R.A.E., May 1950.

TABLE I.- VALUES OF EXPERIMENTAL PRESSURE COEFFICIENT

[Uncorrected for basic loading due to spanwise variation of tunnel stream angle; R = 4,000,000]

Orifice location		Pressure coefficient, S							
$\frac{x}{c}$	$\frac{z}{c}$	$\frac{2y}{b}$ = 0	$\frac{2y}{b}$ = 0.03	$\frac{2y}{b}$ = 0.10	$\frac{2y}{b}$ = 0.30	$\frac{2y}{b}$ = 0.55	$\frac{2y}{b}$ = 0.75	$\frac{2y}{b}$ = 0.90	$\frac{2y}{b}$ = 0.96
				α = -0.4°					
0	0	0	0.48	0.59	0.64	0.64	0.59	0.55	0.64
.001	.0045	.13	-----	.65	.67	.68	.62	.57	.59
.0025	.0069	.24	----	.67	.78	.72	.63	.63	.65
.0050	.0093	.42	----	.83	.86	.84	.72	.72	.72
.0125	.0149	.64	.89	.94	1.01	.97	.89	.88	.90
.0250	.0208	.77	.96	1.04	1.10	1.07	.99	.99	1.00
.050	.0290	.90	1.04	1.12	1.23	1.16	1.10	1.09	1.12
.085	.0371	.99	1.09	1.17	1.21	1.20	1.15	1.14	1.17
.15	.0475	1.06	1.16	1.22	1.26	1.25	1.21	1.20	1.23
.25	.0566	1.18	1.22	1.27	1.29	1.28	1.25	1.25	1.25
.35	.0600	1.23	1.23[a]	1.28	1.29	1.28	1.25	1.25	1.24
.45	.0579	1.25	1.23[a]	1.26	1.26	1.25	1.23	1.22	1.21
.55	.0515	1.25	-----	1.22	1.21	----	1.18	1.17	1.15
.65	.0419	1.22	1.16[a]	1.15	1.15	1.13	1.11	1.11	1.08
.75	.0303	1.16	----	1.09	1.08	1.07	1.05	1.04	1.02
.85	.0183	1.09	----	1.03	1.03	1.02	.99	.99	.97
.95	.0063	1.03	.89[a]	.96	.97	.95	.93	.92	.91
.0125	-.0149	.64	.97	.95	.95	1.06	1.08	1.06	1.06
.0250	-.0208	----	1.06	----	----	----	----	----	----
.0375	-.0254	.85	----	----	1.12	1.22	1.22	1.20	1.21
.050	-.0290	----	1.11	----	----	----	----	----	----
.075	-.0350	.98	----	1.15	1.19	1.28	1.26	1.24	1.25
.085	-.0371	----	1.11	----	----	----	----	----	----
.15	-.0475	1.08	1.16	1.23	1.26	1.34	1.31	1.29	1.29
.25	-.0566	1.19	1.22[a]	1.28	----	1.36	1.32	1.30	1.28
.35	-.0600	1.24	----	1.28	1.31	1.35	1.31	1.29	1.27
.45	-.0579	1.26	1.26[a]	1.27	1.30	1.30	1.28	1.26	1.23
.55	-.0515	1.27	----	1.23	1.26	1.22	1.21	1.20	1.16
.65	-.0419	1.23	1.18[a]	1.16	----	1.15	1.14	1.11	1.08
.75	-.0303	1.17	----	1.09	1.13	1.08	1.06	1.04	1.01
.85	-.0183	1.11	----	1.03	1.06	1.02	1.00	.99	.96
.95	-.0063	1.02	.85[a]	.96	.97	.94	.93	.92	.90
				α = 0.6°					
0	0	0.01	0.56	0.64	0.65	0.62	0.61	0.57	0.60
.001	.0045	.16	-----	.75	.78	.77	.72	.67	.65
.0025	.0069	.29	----	.88	.89	.84	.76	.77	.77
.0050	.0093	.46	----	.95	1.01	.99	.89	.90	.84
.0125	.0149	.69	.98	1.08	1.16	1.12	1.01	1.06	1.04
.0250	.0208	.83	1.04	1.16	1.24	1.19	1.13	1.13	1.14
.050	.0290	.95	1.11	1.20	1.26	1.26	1.21	1.21	1.22
.085	.0371	1.04	1.15	1.24	1.30	1.29	1.24	1.24	1.25
.15	.0475	1.12	1.20	1.28	1.33	1.31	1.28	1.28	1.29
.25	.0566	1.22	1.27	1.31	1.34	1.33	1.31	1.31	1.30
.35	.0600	1.26	1.28[a]	1.31	1.33	1.32	1.29	1.29	1.27
.45	.0579	1.29	1.27[a]	1.29	1.28	1.28	1.26	1.26	1.23
.55	.0515	1.28	----	1.24	1.23	----	1.20	1.20	1.17
.65	.0419	1.25	1.21[a]	1.17	1.16	1.15	1.13	1.13	1.09
.75	.0303	1.19	----	1.10	1.09	1.08	1.06	1.06	1.02
.85	.0183	1.11	----	1.04	1.04	1.02	1.00	1.00	.97
.95	.0063	1.04	.94[a]	.96	.97	.95	.93	.93	.91
.0125	-.0149	.60	.80	.85	.83	.91	.92	.91	.93
.0250	-.0208	----	.90	----	----	----	----	----	----
.0375	-.0254	.80	----	----	1.01	1.10	1.09	1.08	1.10
.050	-.0290	----	1.00	----	----	----	----	----	----
.075	-.0350	.93	----	1.10	1.10	1.18	1.16	1.15	1.17
.085	-.0371	----	1.06	----	----	----	----	----	----
.15	-.0475	1.04	1.12	1.18	1.19	1.26	1.23	1.22	1.24
.25	-.0566	1.15	1.19[a]	1.23	----	1.30	1.27	1.26	1.26
.35	-.0600	1.21	----	1.25	1.28	1.30	1.26	1.26	1.25
.45	-.0579	1.24	1.25[a]	1.25	1.27	1.26	1.24	1.22	1.21
.55	-.0515	1.24	----	1.21	1.23	1.21	1.19	1.19	1.16
.65	-.0419	1.20	1.18[a]	1.15	----	1.14	1.12	1.10	1.08
.75	-.0303	1.15	----	1.08	1.11	1.06	1.05	1.03	1.02
.85	-.0183	1.10	----	1.03	1.05	1.01	.99	.98	.96
.95	-.0063	1.02	.96[a]	.96	.97	.94	.93	.92	.90

[a]These pressures measured with static-pressure survey tube about 0.0035c from wing surface.

NACA

TABLE I.- VALUES OF EXPERIMENTAL PRESSURE COEFFICIENT - Continued

[Uncorrected for basic loading due to spanwise variation of tunnel stream angle; R = 4,000,000]

Orifice location		Pressure coefficient, S							
$\frac{x}{c}$	$\frac{z}{c}$	$\frac{2y}{b}$ = 0	$\frac{2y}{b}$ = 0.03	$\frac{2y}{b}$ = 0.10	$\frac{2y}{b}$ = 0.30	$\frac{2y}{b}$ = 0.55	$\frac{2y}{b}$ = 0.75	$\frac{2y}{b}$ = 0.90	$\frac{2y}{b}$ = 0.96
α = 2.7°									
0	0	0.03	0.61	0.78	0.93	0.92	0.81	0.74	0.81
.001	.0045	.25	----	1.03	1.22	1.22	1.13	1.04	.93
.0025	.0069	.39	----	1.12	1.36	1.33	1.22	1.22	1.19
.0050	.0093	.60	----	1.28	1.49	1.49	1.30	1.35	1.26
.0125	.0149	.82	1.18	1.39	1.59	1.59	1.44	1.45	1.46
.0250	.0208	.94	1.20	1.38	1.56	1.54	1.48	1.48	1.48
.050	.0290	1.06	1.24	1.39	1.46	1.53	1.48	1.48	1.48
.085	.0371	1.13	1.26	1.38	1.49	1.49	1.45	1.45	1.45
.15	.0475	1.20	1.29	1.39	1.47	1.47	1.44	1.44	1.45
.25	.0566	1.29	1.34	1.40	1.44	1.45	1.42	1.42	1.39
.35	.0600	1.33	1.34[a]	1.38	1.40	1.40	1.38	1.38	1.33
.45	.0579	1.35	1.32[a]	1.35	1.34	1.33	1.32	1.32	1.27
.55	.0515	1.33	----	1.28	1.27	----	1.24	1.23	1.19
.65	.0419	1.28	1.25[a]	1.20	1.19	1.18	1.16	1.15	1.10
.75	.0303	1.22	----	1.12	1.11	1.10	1.08	1.07	1.03
.85	.0183	1.13	----	1.05	1.04	1.03	1.01	1.01	.97
.95	.0063	1.04	.95[a]	.96	.97	.95	.93	.93	.92
.0125	-.0149	.50	.66	.68	.64	.69	.67	.68	.71
.0250	-.0208	----	.89	----	----	----	----	----	----
.0375	-.0254	.71	----	----	.82	.89	.86	.86	.90
.050	-.0290	----	.96	----	----	----	----	----	----
.075	-.0350	.84	----	.96	.94	1.00	.97	.97	1.01
.085	-.0371	----	.96	----	----	----	----	----	----
.15	-.0475	.96	1.03	1.06	1.06	1.12	1.09	1.09	1.12
.25	-.0566	1.07	1.12[a]	1.14	----	1.19	1.15	1.16	1.18
.35	-.0600	1.13	----	1.17	1.19	1.21	1.17	1.17	1.19
.45	-.0579	1.17	1.19[a]	1.18	1.20	1.20	1.17	1.17	1.17
.55	-.0515	1.18	----	1.15	1.18	1.16	1.13	1.13	1.14
.65	-.0419	1.15	1.14[a]	1.11	----	1.17	1.08	1.08	1.08
.75	-.0303	1.11	----	1.05	1.09	1.04	1.03	1.02	1.02
.85	-.0183	1.07	----	1.00	1.03	1.00	.98	.97	.97
.95	-.0063	1.00	.95[a]	.95	.97	.94	.93	.92	.92
α = 3.7°									
0	0	0.04	0.73	0.88	1.13	1.10	1.06	1.02	1.03
.001	.0045	.29	----	1.16	1.48	1.50	1.49	1.42	1.25
.0025	.0069	.44	----	1.29	1.66	1.62	1.57	1.62	1.52
.0050	.0093	.65	----	1.41	1.74	1.75	1.64	1.74	1.62
.0125	.0149	.87	1.29	1.51	1.83	1.81	1.69	1.72	1.70
.0250	.0208	.99	1.28	1.51	1.74	1.73	1.69	1.68	1.68
.050	.0290	1.10	1.31	1.48	1.57	1.68	1.63	1.63	1.62
.085	.0371	1.17	1.30	1.46	1.58	1.61	1.57	1.56	1.54
.15	.0475	1.24	1.34	1.44	1.54	1.56	1.58	1.51	1.49
.25	.0566	1.33	1.38	1.44	1.49	1.50	1.49	1.47	1.42
.35	.0600	1.36	----	1.41	1.44	1.44	1.42	1.40	1.35
.45	.0579	1.36	----	1.36	1.37	1.37	1.35	1.33	1.28
.55	.0515	1.35	----	1.29	1.29	----	1.27	1.24	1.19
.65	.0419	1.30	----	1.21	1.20	1.20	1.17	1.15	1.10
.75	.0303	1.23	----	1.12	1.12	1.11	1.09	1.06	1.02
.85	.0183	1.14	----	1.04	1.05	1.03	1.01	1.00	.96
.95	.0063	1.04	----	.96	.97	.95	.93	.92	.91
.0125	-.0149	.44	.61	.62	.59	.64	.61	.61	.63
.0250	-.0208	----	.71	----	----	----	----	----	----
.0375	-.0254	.65	----	----	.75	.81	.78	.77	.80
.050	-.0290	----	.84	----	----	----	----	----	----
.075	-.0350	.79	----	.91	.87	.94	.90	.89	.93
.085	-.0371	----	.90	----	----	----	----	----	----
.15	-.0475	.91	.98	1.02	1.00	1.07	1.03	1.02	1.06
.25	-.0566	1.03	----	1.10	----	1.15	1.11	1.10	1.13
.35	-.0600	1.10	----	1.14	1.15	1.19	1.14	1.13	1.15
.45	-.0579	1.14	----	1.15	1.16	1.18	1.13	1.14	1.14
.55	-.0515	1.15	----	1.13	1.14	1.15	1.12	1.11	1.12
.65	-.0419	1.13	----	1.09	----	1.10	1.08	1.06	1.06
.75	-.0303	1.09	----	1.04	1.07	1.04	1.02	1.02	1.01
.85	-.0183	1.05	----	1.00	1.03	1.00	.98	.97	.97
.95	-.0063	.99	----	.94	.96	.94	.94	.92	.91

[a]These pressures measured with static-pressure survey tube about 0.0035c from wing surface.

TABLE I.- VALUES OF EXPERIMENTAL PRESSURE COEFFICIENT - Continued

[Uncorrected for basic loading due to spanwise variation of tunnel stream angle; R = 4,000,000]

Orifice location		Pressure coefficient, S							
$\frac{x}{c}$	$\frac{z}{c}$	$\frac{2y}{b}$ = 0	$\frac{2y}{b}$ = 0.03	$\frac{2y}{b}$ = 0.10	$\frac{2y}{b}$ = 0.30	$\frac{2y}{b}$ = 0.55	$\frac{2y}{b}$ = 0.75	$\frac{2y}{b}$ = 0.90	$\frac{2y}{b}$ = 0.96
$\alpha = 4.7°$									
0	0	0.07	0.75	1.06	1.38	1.37	1.35	1.25	1.24
.001	.0045	.34	----	1.41	1.78	1.81	1.83	1.72	1.52
.0025	.0069	.50	----	1.52	1.94	1.93	1.90	1.91	1.84
.0050	.0093	.72	----	1.66	2.00	2.03	1.94	2.02	1.87
.0125	.0149	.94	1.42	1.71	2.05	2.08	1.99	2.02	1.98
.0250	.0208	1.06	1.39	1.66	1.94	1.94	1.93	1.90	1.90
.050	.0290	1.16	1.39	1.59	1.72	1.84	1.80	1.80	1.77
.085	.0371	1.23	1.37	1.54	1.68	1.72	1.70	1.68	1.65
.15	.0475	1.29	1.39	1.51	1.61	1.62	1.61	1.59	1.56
.25	.0566	1.36	1.41	1.48	1.54	1.55	1.54	1.52	1.47
.35	.0600	1.39	1.40[a]	1.44	1.48	1.48	1.46	1.45	1.39
.45	.0579	1.40	1.36[a]	1.39	1.40	1.40	1.38	1.36	1.30
.55	.0515	1.37	----	1.32	1.31	----	1.29	1.26	1.21
.65	.0419	1.32	1.28[a]	1.22	1.21	1.20	1.18	1.16	1.12
.75	.0303	1.25	----	1.13	1.12	1.11	1.09	1.07	1.03
.85	.0183	1.15	----	1.05	1.05	1.03	1.01	1.00	.97
.95	.0063	1.05	.99[a]	.96	.97	.95	.93	.93	.92
.0125	-.0149	.40	.56	.58	.56	.60	.57	.57	.60
.0250	-.0208	----	.66	----	----	----	----	----	----
.0375	-.0254	.61	----	----	.68	.74	.70	.70	.74
.050	-.0290	----	.79	----	----	----	----	----	----
.075	-.0350	.75	----	.85	.81	.86	.83	.83	.87
.085	-.0371	----	.85	----	----	----	----	----	----
.15	-.0475	.88	.94	.97	.95	1.01	.97	.97	1.02
.25	-.0566	1.00	1.04[a]	1.06	----	1.11	1.06	1.06	1.11
.35	-.0600	1.06	----	1.11	1.12	1.15	1.11	1.10	1.14
.45	-.0579	1.11	1.12[a]	1.13	1.14	1.15	1.12	1.12	1.14
.55	-.0515	1.13	----	1.11	1.13	1.13	1.10	1.10	1.11
.65	-.0419	1.11	1.09[a]	1.08	----	1.08	1.06	1.06	1.07
.75	-.0303	1.08	----	1.03	1.07	1.03	1.02	1.01	1.02
.85	-.0183	1.04	----	.99	1.03	1.00	.98	.98	.98
.95	-.0063	.99	.92[a]	.95	.98	.95	.94	.93	.93
$\alpha = 6.8°$									
0	0	0.11	0.96	1.51	2.06	2.07	2.07	1.96	1.93
.001	.0045	.45	----	1.93	2.56	2.62	2.69	2.57	2.27
.0025	.0069	.63	----	2.01	2.74	2.71	2.74	2.81	2.70
.0050	.0093	.85	----	2.15	2.69	2.77	2.69	2.77	2.67
.0125	.0149	1.07	1.69	2.10	2.64	2.69	2.58	2.63	2.56
.0250	.0208	1.17	1.59	1.96	2.38	2.38	2.40	2.36	2.35
.050	.0290	1.26	1.53	1.80	1.99	2.12	2.10	2.09	2.04
.085	.0371	1.32	1.49	1.68	1.90	1.93	1.91	1.89	1.84
.15	.0475	1.37	1.47	1.62	1.76	1.79	1.77	1.75	1.69
.25	.0566	1.43	1.48	1.57	1.64	1.66	1.64	1.62	1.54
.35	.0600	1.45	1.46[a]	1.51	1.55	1.55	1.53	1.51	1.43
.45	.0579	1.45	1.41[a]	1.44	1.45	1.45	1.43	1.40	1.32
.55	.0515	1.41	----	1.35	1.34	----	1.31	1.27	1.21
.65	.0419	1.35	1.33[a]	1.24	1.23	1.21	1.19	1.16	1.11
.75	.0303	1.27	----	1.14	1.13	1.11	1.08	1.06	1.02
.85	.0183	1.17	----	1.05	1.05	1.03	1.01	.99	.96
.95	.0063	1.05	1.00[a]	.96	.98	.96	.95	.93	.92
.0125	-.0149	.31	.50	.54	.58	.66	.57	.57	.60
.0250	-.0208	----	.57	----	----	----	----	----	----
.0375	-.0254	.52	----	----	.60	.65	.60	.60	.65
.050	-.0290	----	.70	----	----	----	----	----	----
.075	-.0350	.66	----	.75	.71	.76	.72	.72	.77
.085	-.0371	----	.76	----	----	----	----	----	----
.15	-.0475	.80	.86	.88	.85	.92	.87	.86	.93
.25	-.0566	.92	1.06[a]	.99	----	1.06	.98	.98	1.04
.35	-.0600	.99	----	1.04	1.04	1.09	1.04	1.04	1.09
.45	-.0579	1.05	1.07[a]	1.06	1.08	1.10	1.05	1.06	1.10
.55	-.0515	1.06	----	1.05	1.08	1.09	1.05	1.05	1.08
.65	-.0419	1.05	1.06[a]	1.04	----	1.06	1.04	1.04	1.05
.75	-.0303	1.04	----	1.00	1.04	1.02	1.00	1.01	1.03
.85	-.0183	1.01	----	.97	1.02	.98	.97	.98	.99
.95	-.0063	.96	.90[a]	.95	.97	.96	.95	.95	.94

[a]These pressures measured with static-pressure survey tube about 0.0035c from wing surface.

NACA

TABLE I.- VALUES OF EXPERIMENTAL PRESSURE COEFFICIENT - Continued

[Uncorrected for basic loading due to spanwise variation of tunnel stream angle; R = 4,000,000]

Orifice location		Pressure coefficient, S							
$\frac{x}{c}$	$\frac{z}{c}$	$\frac{2y}{b}$ = 0	$\frac{2y}{b}$ = 0.03	$\frac{2y}{b}$ = 0.10	$\frac{2y}{b}$ = 0.30	$\frac{2y}{b}$ = 0.55	$\frac{2y}{b}$ = 0.75	$\frac{2y}{b}$ = 0.90	$\frac{2y}{b}$ = 0.96
α = 5.8°									
0	0	0.18	1.26	2.00	2.89	2.93	3.00	2.84	2.71
.001	.0045	.57	----	2.49	3.49	3.50	3.65	3.58	3.15
.0025	.0069	.76	----	2.58	3.61	3.60	3.69	3.84	3.60
.0050	.0093	1.00	----	2.64	3.44	3.57	3.51	3.61	3.48
.0125	.0149	1.21	1.97	2.50	3.26	3.30	3.26	3.30	3.21
.0250	.0208	1.29	1.79	2.27	2.82	2.83	2.90	2.82	2.82
.050	.0290	1.37	1.69	1.99	2.27	2.46	2.42	2.41	2.33
.085	.0371	1.41	1.59	1.84	2.10	2.16	2.14	2.12	2.04
.15	.0475	1.44	1.58	1.73	1.90	1.94	1.88	1.90	1.82
.25	.0566	1.50	1.55	1.64	1.73	1.76	1.74	1.71	1.62
.35	.0600	1.51	1.53[a]	1.56	1.61	1.62	1.59	1.56	1.47
.45	.0579	1.50	1.46[a]	1.48	1.48	1.48	1.45	1.41	1.34
.55	.0515	1.45	----	1.37	1.35	----	1.31	1.26	1.21
.65	.0419	1.39	1.34[a]	1.26	1.23	1.21	1.18	1.13	1.09
.75	.0303	1.29	----	1.15	1.12	1.10	1.08	1.05	1.01
.85	.0183	1.18	----	1.05	1.05	1.04	1.03	1.01	.98
.95	.0063	1.06	1.01[a]	.96	.99	1.00	1.00	.99	.97
.0125	-.0149	.25	.48	.56	.66	.68	.66	.64	.67
.0250	-.0208	----	.51	----	----	----	----	----	----
.0375	-.0254	.45	----	----	.55	.59	.56	.56	.60
.050	-.0290	----	.63	----	----	----	----	----	----
.075	-.0350	.60	----	.67	.63	.68	.64	.64	.70
.085	-.0371	----	.69	----	----	----	----	----	----
.15	-.0475	.73	.79	.80	.77	.83	.78	.79	.86
.25	-.0566	.86	.89[a]	.92	----	.95	.91	.91	.99
.35	-.0600	.93	----	.98	.98	1.03	.98	.99	1.06
.45	-.0579	.99	1.01[a]	1.02	1.02	1.05	1.02	1.03	1.09
.55	-.0515	1.02	----	1.02	1.04	1.06	1.03	1.04	1.09
.65	-.0419	1.01	1.00[a]	1.01	----	1.06	1.02	1.03	1.07
.75	-.0303	1.00	----	.98	1.02	1.01	1.00	1.01	1.04
.85	-.0183	.98	----	.96	1.00	.99	.98	.99	1.02
.95	-.0063	.95	.89[a]	.94	.98	.98	.98	.98	.99
α = 12.9°									
0	0	0.38	2.01	3.55	5.32	5.43	4.95	4.16	3.67
.001	.0045	.89	----	4.10	6.05	6.03	5.66	5.05	4.13
.0025	.0069	1.10	----	4.08	5.99	6.03	5.56	5.20	4.53
.0050	.0093	1.33	----	4.00	5.46	5.60	5.10	4.68	4.25
.0125	.0149	1.52	2.62	3.58	4.88	4.98	4.43	4.13	3.82
.0250	.0208	1.57	2.30	2.99	3.87	3.86	3.71	3.29	3.11
.050	.0290	1.60	2.04	2.52	2.98	3.17	2.93	2.64	2.42
.085	.0371	1.62	1.87	2.22	2.69	2.62	2.45	2.19	1.98
.15	.0475	1.62	1.76	1.99	2.23	2.22	2.05	1.78	1.58
.25	.0566	1.65	1.71	1.83	1.94	1.89	1.68	1.41	1.27
.35	.0600	1.63	1.65[a]	1.70	1.74	1.64	1.40	1.30	1.20
.45	.0579	1.60	1.51[a]	1.58	1.56	1.38	1.29	1.28	1.18
.55	.0515	1.54	----	1.44	1.38	----	1.27	1.27	1.17
.65	.0419	1.45	1.39[a]	1.30	1.25	1.24	1.27	1.27	1.19
.75	.0303	1.34	----	1.19	1.16	1.22	1.28	1.29	1.18
.85	.0183	1.21	----	1.07	1.12	1.23	1.33	1.31	1.20
.95	.0063	1.07	1.01[a]	.98	1.09	1.24	1.32	1.30	1.21
.0125	-.0149	.11	.51	.74	1.11	1.09	1.01	.87	.85
.0250	-.0208	----	.43	----	----	----	----	----	----
.0375	-.0254	.30	----	----	.57	.61	.57	.55	.58
.050	-.0290	----	.50	----	----	----	----	----	----
.075	-.0350	.44	----	.53	.53	.58	.55	.56	.62
.085	-.0371	----	.54	----	----	----	----	----	----
.15	-.0475	.57	.63	.65	.63	.69	.66	.69	.78
.25	-.0566	.71	.74[a]	.77	----	.83	.80	.84	.93
.35	-.0600	.80	----	.85	.85	.92	.90	.93	1.02
.45	-.0579	.86	.88[a]	.90	.91	.98	.96	1.01	1.07
.55	-.0515	.90	----	.92	.95	1.01	1.00	1.04	1.09
.65	-.0419	.91	.91[a]	.92	----	1.01	1.01	1.06	1.08
.75	-.0303	.91	----	.92	.97	1.01	1.02	1.06	1.08
.85	-.0183	.91	----	.92	.99	1.03	1.05	1.09	1.09
.95	-.0063	.89	.93[a]	.92	1.01	1.07	1.11	1.14	1.13

[a]These pressures measured with static-pressure survey tube about 0.0035c from wing surface.

NACA

TABLE I.- VALUES OF EXPERIMENTAL PRESSURE COEFFICIENT - Continued

[Uncorrected for basic loading due to spanwise variation of tunnel stream angle; R = 4,000,000]

Orifice location		Pressure coefficient, S							
$\frac{x}{c}$	$\frac{z}{c}$	$\frac{2y}{b}$ = 0	$\frac{2y}{b}$ = 0.03	$\frac{2y}{b}$ = 0.10	$\frac{2y}{b}$ = 0.30	$\frac{2y}{b}$ = 0.55	$\frac{2y}{b}$ = 0.75	$\frac{2y}{b}$ = 0.90	$\frac{2y}{b}$ = 0.96
α = 15.9°									
0	0	0.57	2.78	5.03	7.60	7.55	4.57	2.92	2.92
.001	.0045	1.16	----	5.56	8.39	8.06	4.95	3.44	3.20
.0025	.0069	1.36	----	5.44	8.11	7.98	4.85	3.46	3.45
.0050	.0093	1.60	----	5.18	7.28	7.20	4.35	3.08	3.25
.0125	.0149	1.77	3.21	4.45	6.12	6.08	3.59	2.66	2.81
.0250	.0208	1.78	2.63	3.64	4.78	4.63	2.73	2.03	2.23
.050	.0290	1.78	2.31	2.93	3.56	3.61	1.82	1.51	1.63
.085	.0371	1.77	2.06	2.51	3.00	2.87	1.62	1.36	1.34
.15	.0475	1.75	1.91	2.18	2.47	2.29	1.56	1.33	1.28
.25	.0566	1.75	1.81	1.95	2.07	1.78	1.53	1.31	1.25
.35	.0600	1.72	1.74[a]	1.78	1.81	1.57	1.52	1.31	1.24
.45	.0579	1.68	1.59[a]	1.64	1.58	1.52	1.53	1.31	1.24
.55	.0515	1.60	----	1.48	1.40	----	1.57	1.30	1.24
.65	.0419	1.50	1.43[a]	1.33	1.30	1.53	1.69	1.30	1.23
.75	.0303	1.37	----	1.20	1.26	1.58	1.75	1.29	1.22
.85	.0183	1.23	----	1.09	1.24	1.64	1.64	1.28	1.21
.95	.0063	1.07	1.01[a]	1.00	1.22	1.45	1.51	1.26	1.20
.0125	-.0149	.06	.63	1.02	1.64	1.54	1.01	.74	.79
.0250	-.0208	----	.45	----	----	----	----	----	----
.0375	-.0254	.21	----	----	.68	.69	.54	.53	.58
.050	-.0290	----	.47	----	----	----	----	----	----
.075	-.0350	.34	----	.48	.51	.54	.50	.56	.63
.085	-.0371	----	.55	----	----	----	----	----	----
.15	-.0475	.48	.58	.56	.55	.61	.61	.69	.77
.25	-.0566	.61	.64[a]	.68	----	.74	.76	.83	.92
.35	-.0600	.70	----	.76	.76	.85	.87	.94	1.01
.45	-.0579	.77	.79[a]	.82	.83	.92	.95	1.02	1.07
.55	-.0515	.82	----	.85	.88	.97	1.01	1.06	1.09
.65	-.0419	.84	.83[a]	.87	----	.99	1.04	1.08	1.10
.75	-.0303	.85	----	.87	.93	1.01	1.07	1.09	1.09
.85	-.0183	.85	----	.88	.96	1.05	1.13	1.11	1.11
.95	-.0063	.85	.80[a]	.91	1.02	1.14	1.26	1.16	1.14
α = 17.0°									
0	0	.65	3.30	5.49	8.51	8.15	1.66	2.09	2.59
.001	.0045	1.25	----	6.04	9.34	8.59	1.65	2.14	2.67
.0025	.0069	1.46	----	5.83	8.93	8.45	1.55	1.93	2.40
.0050	.0093	1.71	----	5.52	8.05	7.61	1.55	1.82	2.28
.0125	.0149	1.86	3.48	4.65	6.62	6.29	1.58	1.82	2.24
.0250	.0208	1.85	2.81	3.72	5.11	4.73	1.52	1.79	2.15
.050	.0290	1.83	2.41	2.75	3.76	3.59	1.47	1.75	2.02
.085	.0371	1.82	2.13	2.53	3.14	2.75	1.46	1.72	1.93
.15	.0475	1.79	1.95	2.25	2.55	2.11	1.45	1.69	1.85
.25	.0566	1.78	1.85	1.99	2.12	1.87	1.44	1.63	1.65
.35	.0600	1.75	1.75[a]	1.81	1.83	1.84	1.44	1.60	1.47
.45	.0579	1.70	1.60[a]	1.66	1.59	1.80	1.45	1.55	1.38
.55	.0515	1.62	----	1.50	1.42	----	1.48	1.49	1.35
.65	.0419	1.51	1.45[a]	1.34	1.35	1.87	1.49	1.43	1.31
.75	.0303	1.38	----	1.21	1.32	1.89	1.48	1.37	1.33
.85	.0183	1.24	----	1.10	1.31	1.83	1.45	1.32	1.27
.95	.0063	1.07	1.00[a]	1.01	1.28	1.43	1.41	1.26	1.25
.0125	-.0149	.04	.69	1.15	1.89	1.70	.71	.76	.89
.0250	-.0208	----	.44	----	----	----	----	----	----
.0375	-.0254	.18	----	----	.75	.73	.52	.56	.62
.050	-.0290	----	.42	----	----	----	----	----	----
.075	-.0350	.30	----	.46	.52	.53	.53	.57	.63
.085	-.0371	----	.42	----	----	----	----	----	----
.15	-.0475	.44	.51	.53	.53	.58	.65	.68	.76
.25	-.0566	.57	.61[a]	.64	----	.71	.78	.81	.89
.35	-.0600	.66	----	.72	.73	.82	.88	.91	.98
.45	-.0579	.74	.74[a]	.79	.80	.89	.96	.98	1.03
.55	-.0515	.79	----	.82	.85	.95	1.01	1.02	1.06
.65	-.0419	.81	.80[a]	.84	----	.97	1.05	1.04	1.07
.75	-.0303	.82	----	.85	.92	.99	1.08	1.05	1.07
.85	-.0183	.83	----	.87	.95	1.03	1.13	1.07	1.08
.95	-.0063	.84	.88[a]	.90	1.02	1.12	1.22	1.12	1.13

[a]These pressures measured with static-pressure survey tube about 0.0035c from wing surface.

TABLE I.- VALUES OF EXPERIMENTAL PRESSURE COEFFICIENT - Continued

[Uncorrected for basic loading due to spanwise variation of tunnel stream angle; R = 4,000,000]

Orifice location		Pressure coefficient, S							
$\frac{x}{c}$	$\frac{z}{c}$	$\frac{2y}{b} = 0$	$\frac{2y}{b} = 0.03$	$\frac{2y}{b} = 0.10$	$\frac{2y}{b} = 0.30$	$\frac{2y}{b} = 0.55$	$\frac{2y}{b} = 0.75$	$\frac{2y}{b} = 0.90$	$\frac{2y}{b} = 0.96$
$\alpha = 19.0°$									
0	0	.82	3.78	6.84	10.30	7.23	1.93	1.91	2.49
.001	.0045	1.47	----	7.36	11.18	7.33	1.83	1.87	2.51
.0025	.0069	1.68	----	7.08	10.57	7.09	1.66	1.68	2.25
.0050	.0093	1.92	----	6.60	9.48	6.34	1.58	1.59	2.09
.0125	.0149	2.05	4.06	5.42	7.66	4.50	1.57	1.63	2.07
.0250	.0208	2.00	3.14	4.37	5.77	2.95	1.53	1.62	2.02
.050	.0290	1.96	2.62	3.39	4.18	2.56	1.49	1.59	1.95
.085	.0371	1.93	2.28	2.83	3.42	2.46	1.48	1.57	1.90
.15	.0475	1.88	2.07	2.39	2.74	2.38	1.46	1.55	1.87
.25	.0566	1.85	1.93	2.07	2.22	2.36	1.45	1.54	1.62
.35	.0600	1.81	1.81[a]	1.88	1.89	2.51	1.43	1.53	1.45
.45	.0579	1.75	1.64[a]	1.71	1.65	2.47	1.42	1.51	1.38
.55	.0515	1.66	----	1.54	1.52	----	1.43	1.48	1.36
.65	.0419	1.52	1.48[a]	1.39	1.46	1.96	1.43	1.43	1.33
.75	.0303	1.41	----	1.25	1.45	1.77	1.42	1.39	1.33
.85	.0183	1.25	----	1.13	1.46	1.63	1.40	1.35	1.28
.95	.0063	1.07	.99[a]	1.02	1.38	1.47	1.38	1.30	1.25
.0125	-.0149	.02	.83	1.44	2.37	1.65	.76	.75	.91
.0250	-.0208	----	.47	----	----	----	----	----	----
.0375	-.0254	.13	----	----	.89	.70	.53	.54	.62
.050	-.0290	----	.40	----	----	----	----	----	----
.075	-.0350	.25	----	.45	.55	.50	.52	.55	.62
.085	-.0371	----	.37	----	----	----	----	----	----
.15	-.0475	.38	.45	.48	.50	.54	.62	.65	.73
.25	-.0566	.51	.52[a]	.58	----	.67	.76	.77	.86
.35	-.0600	.61	----	.66	.68	.79	.86	.88	.96
.45	-.0579	.68	.68[a]	.73	.75	.89	.94	.96	1.02
.55	-.0515	.73	----	.77	.81	.95	1.00	1.01	1.05
.65	-.0419	.76	.75[a]	.80	----	.99	1.04	1.04	1.06
.75	-.0303	.78	----	.82	.89	1.02	1.07	1.06	1.07
.85	-.0183	.80	----	.84	.94	1.07	1.12	1.09	1.09
.95	-.0063	.81	.76[a]	.88	1.03	1.18	1.21	1.15	1.14
$\alpha = 21.0°$									
0	0	1.00	4.56	8.33	12.34	2.43	1.63	1.59	1.76
.001	.0045	1.71	----	8.79	13.19	2.37	1.60	1.54	1.74
.0025	.0069	1.92	----	8.40	12.43	2.21	1.52	1.45	1.63
.0050	.0093	2.14	----	7.77	10.95	2.12	1.51	1.42	1.57
.0125	.0149	2.24	4.66	6.19	8.63	2.12	1.53	1.43	1.58
.0250	.0208	2.16	3.48	4.89	6.15	2.13	1.52	1.43	1.57
.050	.0290	2.10	2.83	3.72	4.58	1.97	1.50	1.42	1.55
.085	.0371	2.04	2.44	3.06	3.78	1.86	1.51	1.41	1.54
.15	.0475	1.98	2.18	2.56	3.17	1.78	1.51	1.40	1.54
.25	.0566	1.95	2.04	2.21	2.68	1.74	1.51	1.40	1.45
.35	.0600	1.90	1.89[a]	1.98	2.35	1.75	1.51	1.39	1.39
.45	.0579	1.84	1.66[a]	1.80	2.02	1.76	1.51	1.38	1.37
.55	.0515	1.75	----	1.63	1.80	----	1.50	1.37	1.35
.65	.0419	1.64	1.53[a]	1.46	1.68	1.77	1.50	1.35	1.34
.75	.0303	1.49	----	1.32	1.62	1.72	1.48	1.34	1.32
.85	.0183	1.32	----	1.19	1.59	1.68	1.46	1.33	1.30
.95	.0063	1.12	1.02[a]	1.06	1.42	1.65	1.43	1.31	1.28
.0125	-.0149	.02	1.02	1.80	2.79	.97	.74	.70	.80
.0250	-.0208	----	.54	----	----	----	----	----	----
.0375	-.0254	.10	----	----	.99	.57	.52	.54	.61
.050	-.0290	----	.40	----	----	----	----	----	----
.075	-.0350	.20	----	.46	.54	.51	.52	.55	.63
.085	-.0371	----	.35	----	----	----	----	----	----
.15	-.0475	.32	.40	.45	.45	.60	.63	.66	.75
.25	-.0566	.46	.48[a]	.54	----	.74	.76	.80	.88
.35	-.0600	.55	----	.62	.64	.86	.88	.90	.98
.45	-.0579	.63	.63[a]	.69	.73	.95	.96	.98	1.04
.55	-.0515	.69	----	.74	.80	1.03	1.02	1.03	1.08
.65	-.0419	.72	.72[a]	.78	----	1.08	1.07	1.07	1.09
.75	-.0303	.75	----	.80	.90	1.12	1.10	1.09	1.10
.85	-.0183	.78	----	.84	.96	1.20	1.15	1.13	1.13
.95	-.0063	.82	.76[a]	.89	1.06	1.34	1.25	1.19	1.18

[a]These pressures measured with static-pressure survey tube about 0.0035c from wing surface.

TABLE I.- VALUES OF EXPERIMENTAL PRESSURE COEFFICIENT - Concluded

[Uncorrected for basic loading due to spanwise variation of tunnel stream angle; R = 4,000,000]

Orifice location		Pressure coefficient, S							
$\frac{x}{c}$	$\frac{z}{c}$	$\frac{2y}{b}$ = 0	$\frac{2y}{b}$ = 0.03	$\frac{2y}{b}$ = 0.10	$\frac{2y}{b}$ = 0.30	$\frac{2y}{b}$ = 0.55	$\frac{2y}{b}$ = 0.75	$\frac{2y}{b}$ = 0.90	$\frac{2y}{b}$ = 0.96
α = 31.0°									
0	0	1.87	6.68	3.03	2.24	2.05	1.68	1.55	1.49
.001	.0045	2.63	----	3.03	2.23	2.02	1.65	1.55	1.48
.0025	.0069	2.75	----	3.03	2.23	2.04	1.64	1.53	1.48
.0050	.0093	2.86	----	2.98	2.21	2.03	1.64	1.52	1.46
.0125	.0149	2.75	4.89	2.98	2.19	2.09	1.64	1.54	1.51
.0250	.0208	2.48	3.59	3.00	2.17	2.04	1.64	1.54	1.50
.050	.0290	2.30	3.16	2.98	2.17	1.88	1.62	1.54	1.50
.085	.0371	2.20	3.14	2.98	2.15	1.82	1.63	1.53	1.49
.15	.0475	2.41	3.08	2.97	2.13	1.82	1.63	1.52	1.49
.25	.0566	2.76	2.96	2.95	2.12	1.83	1.63	1.52	1.49
.35	.0600	2.79	2.73[a]	2.91	2.16	1.84	1.63	1.52	1.49
.45	.0579	2.73	2.51[a]	2.85	2.19	1.85	1.63	1.52	1.48
.55	.0515	2.64	----	2.75	2.18	----	1.63	1.51	1.47
.65	.0419	2.52	2.26[a]	2.59	2.10	1.81	1.62	1.50	1.46
.75	.0303	2.34	----	2.37	2.06	1.77	1.61	1.49	1.45
.85	.0183	2.07	----	2.14	2.08	1.72	1.60	1.48	1.43
.95	.0063	1.73	1.55[a]	1.92	2.06	1.68	1.60	1.46	1.41
.0125	-.0149	.13	1.68	1.60	1.37	1.14	.97	.91	.97
.0250	-.0208	----	.75	----	----	----	----	----	----
.0375	-.0254	.01	----	----	.67	.63	.58	.57	.64
.050	-.0290	----	.36	----	----	----	----	----	----
.075	-.0350	.03	----	.38	.44	.49	.46	.49	.58
.085	-.0371	----	.20	----	----	----	----	----	----
.15	-.0475	.11	.21	.31	.40	.50	.49	.52	.64
.25	-.0566	.23	.28[a]	.38	----	.61	.60	.64	.76
.35	-.0600	.34	----	.47	.60	.73	.71	.75	.87
.45	-.0579	.44	.46[a]	.57	.71	.84	.81	.85	.95
.55	-.0515	.53	----	.66	.82	.93	.90	.93	1.01
.65	-.0419	.60	.61[a]	.75	----	1.00	.97	.99	1.05
.75	-.0303	.67	----	.84	1.03	1.06	1.03	1.05	1.08
.85	-.0183	.76	----	.97	1.18	1.16	1.12	1.12	1.14
.95	-.0063	.92	.90[a]	1.23	1.44	1.34	1.29	1.24	1.24

[a]These pressures measured with static-pressure survey tube about 0.0035c from wing surface.

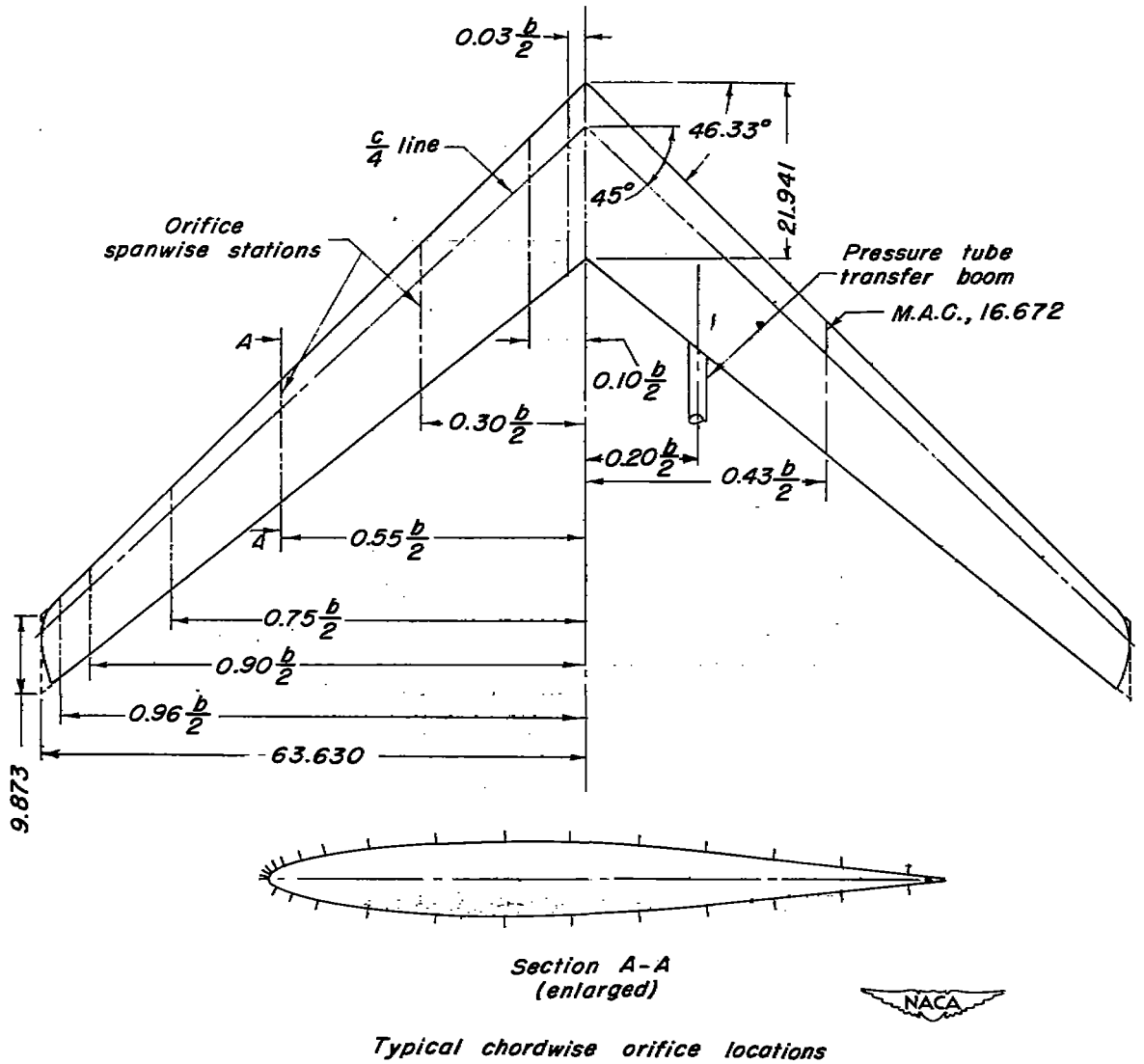

Figure 1.- Geometric characteristics of model. Aspect ratio 8.02; taper ratio 0.45; airfoil section 63_1A012; wing area 14.021 sq ft. (Dimensions in inches except as noted.)

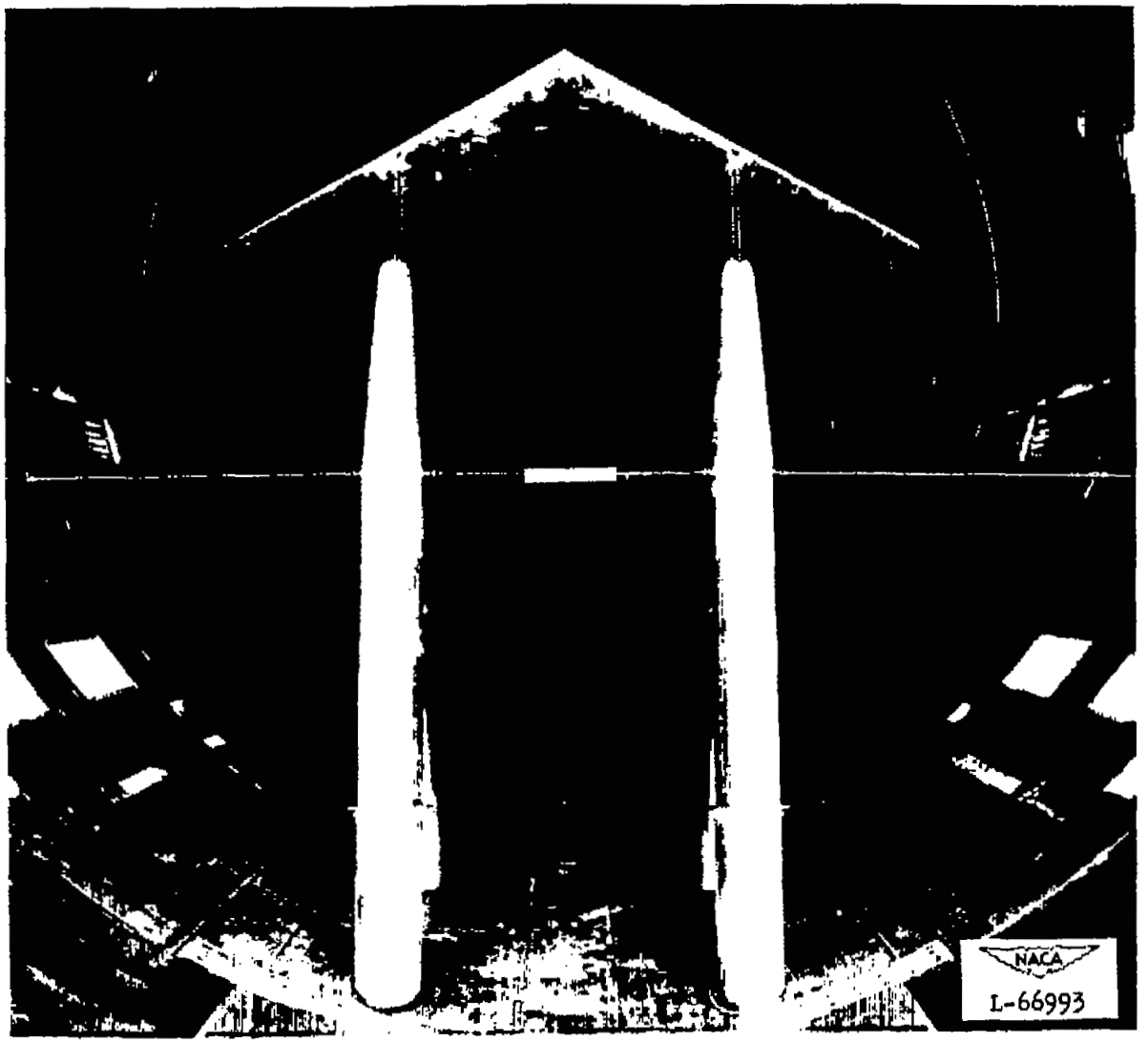

Figure 2.- Model in tunnel for force tests. (Front view.)

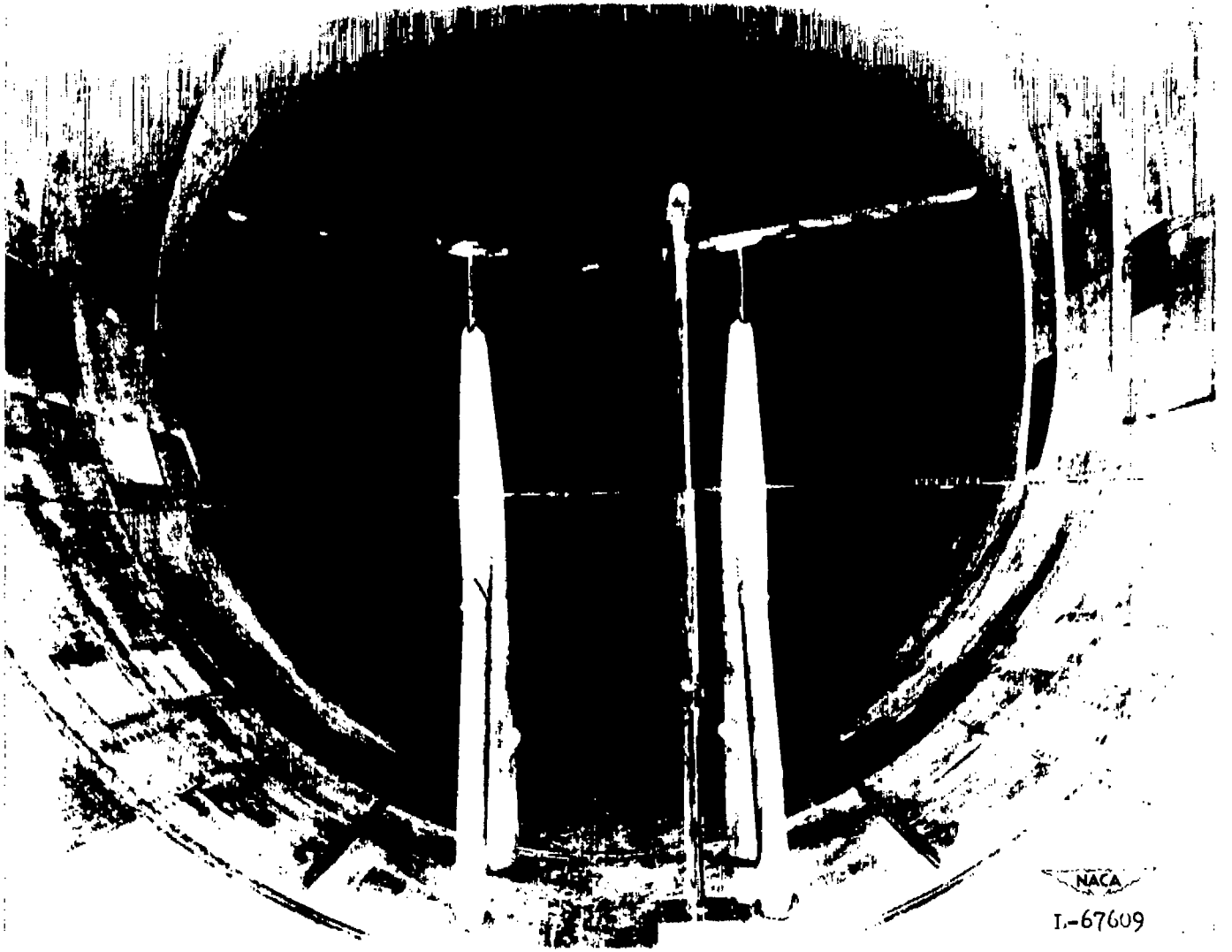

Figure 3.- Model in tunnel for pressure-distribution tests. (Rear view.)

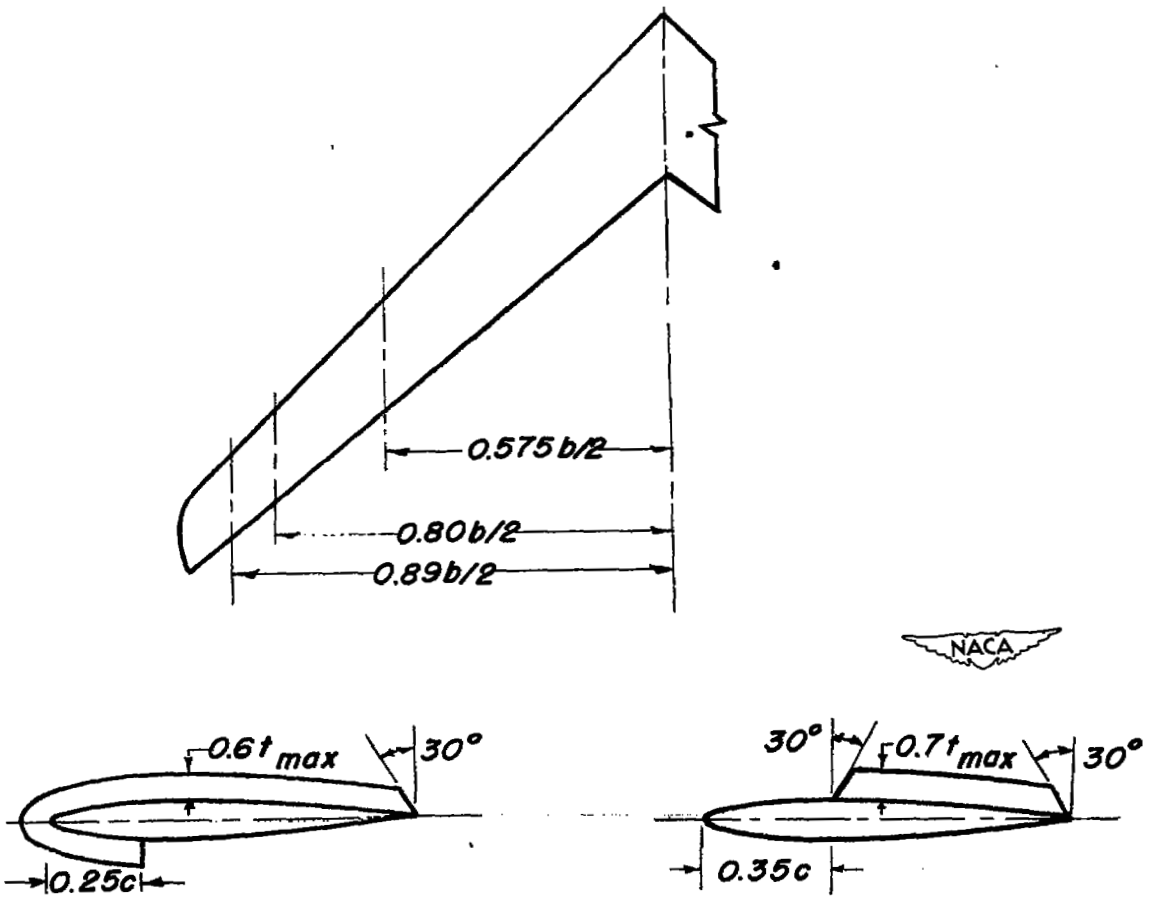

Figure 4.- Details of chordwise fences.

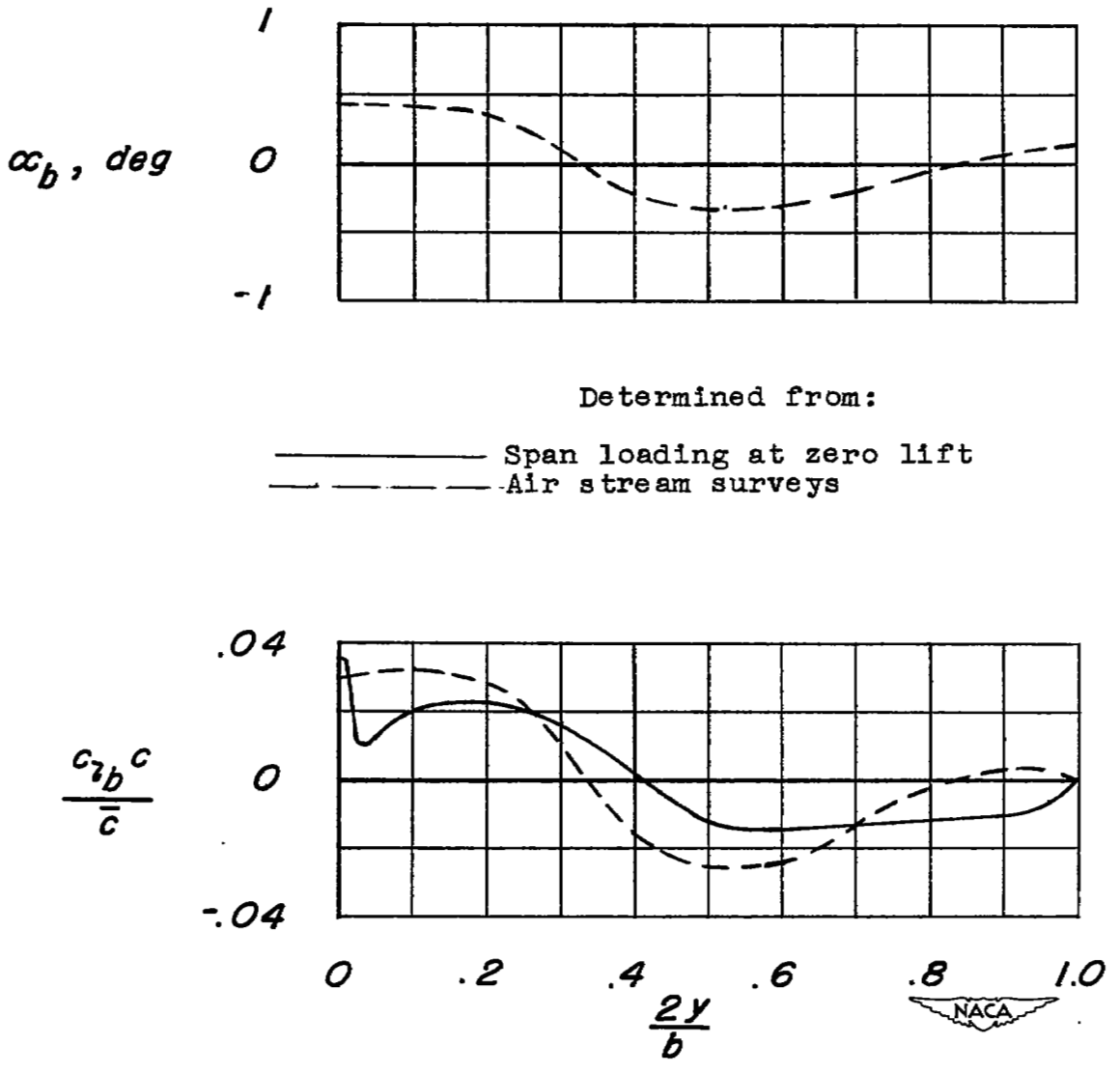

Figure 5.- Basic loading and angle-of-attack distribution across left wing of model.

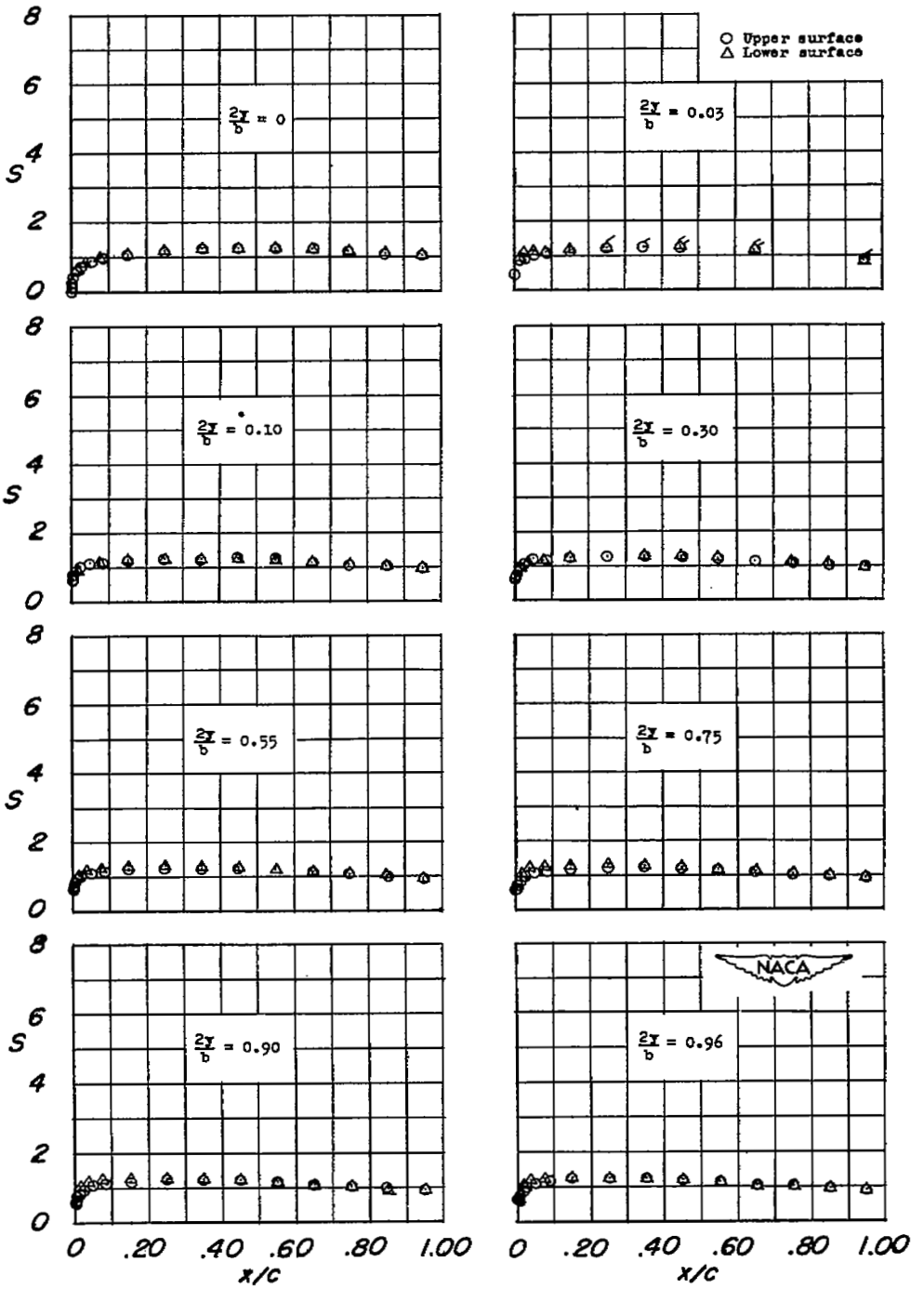

(a) $\alpha = -0.4^{\circ}$.

Figure 6.- Chordwise pressure diagrams for plain wing. R = 4,000,000. (Flagged symbols denote pressures measured with survey tube.)

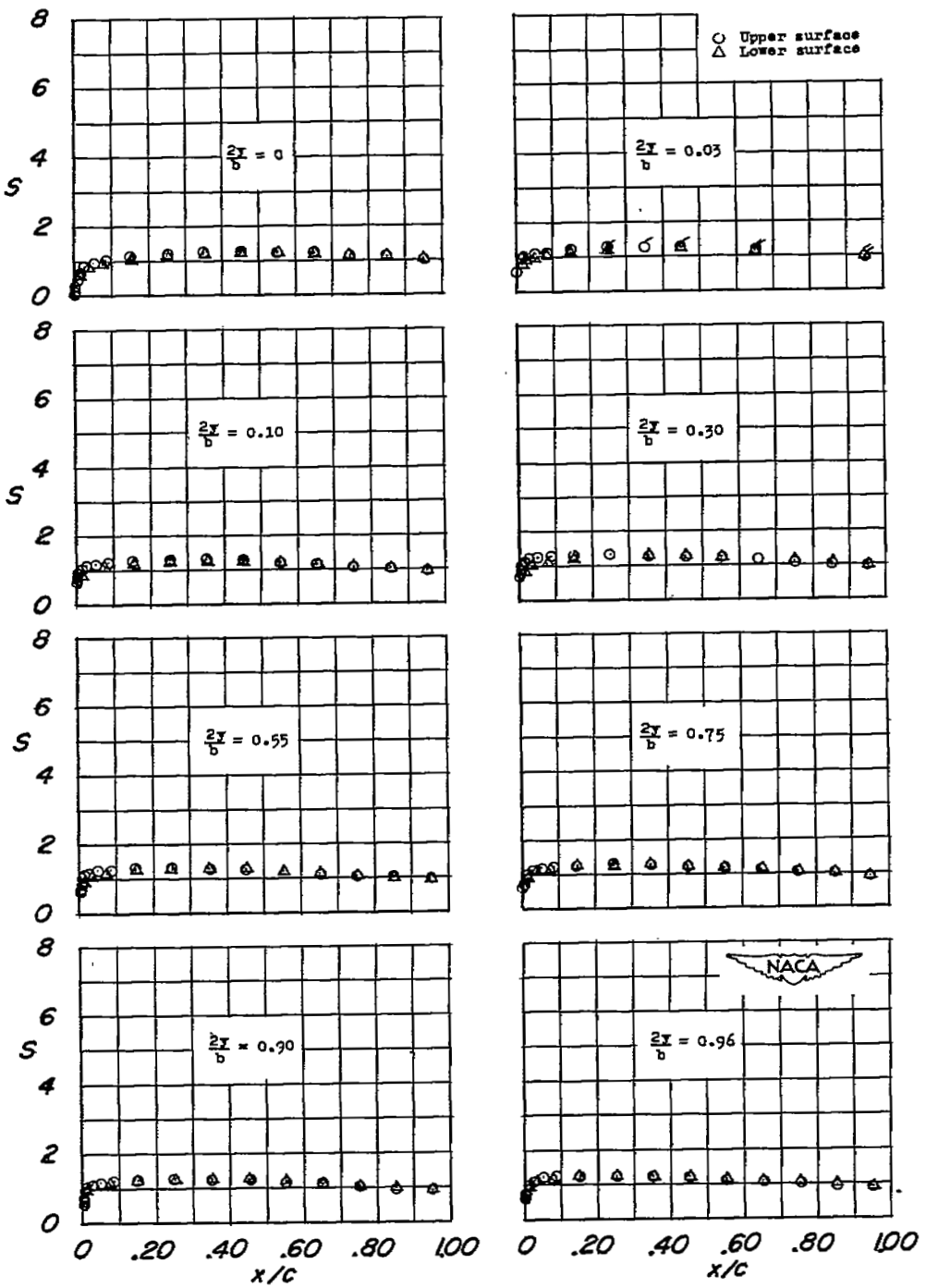

(b) $\alpha = 0.6^{\circ}$.

Figure 6.- Continued.

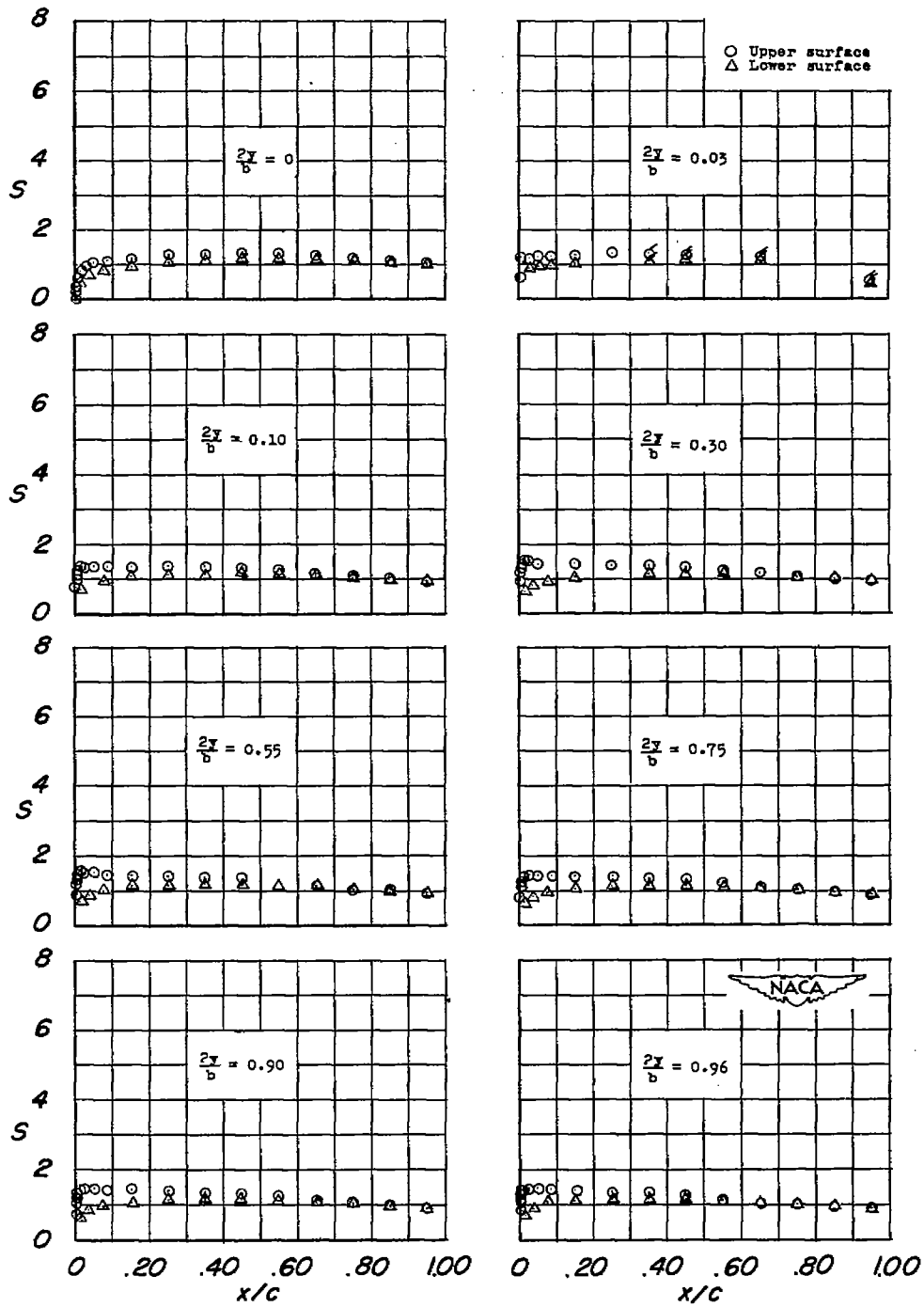

(c) $\alpha = 2.7^{\circ}$.

Figure 6.- Continued.

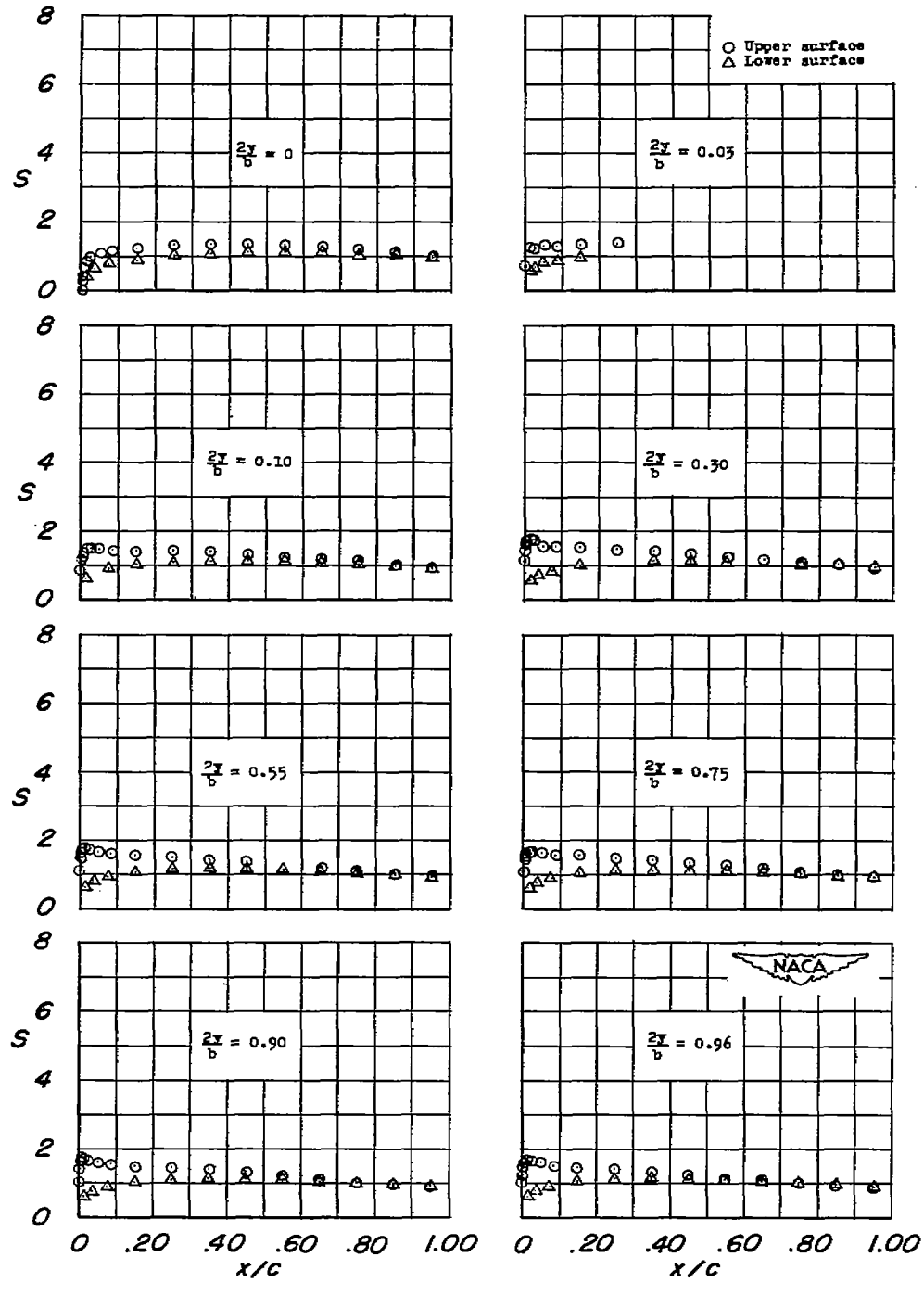

(d) $\alpha = 3.7^{\circ}$.

Figure 6.- Continued.

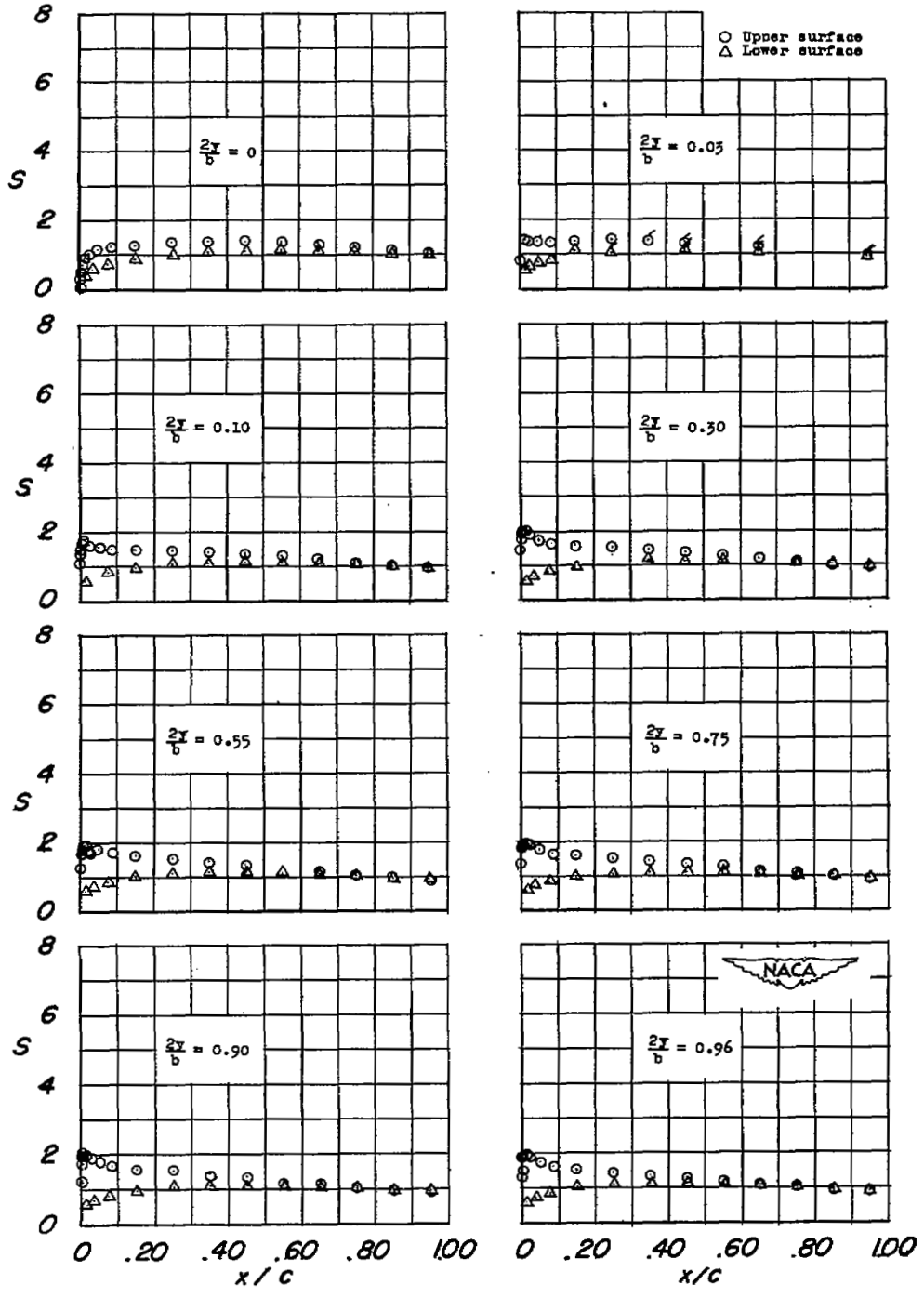

(e) $\alpha = 4.7^{\circ}$.

Figure 6.- Continued.

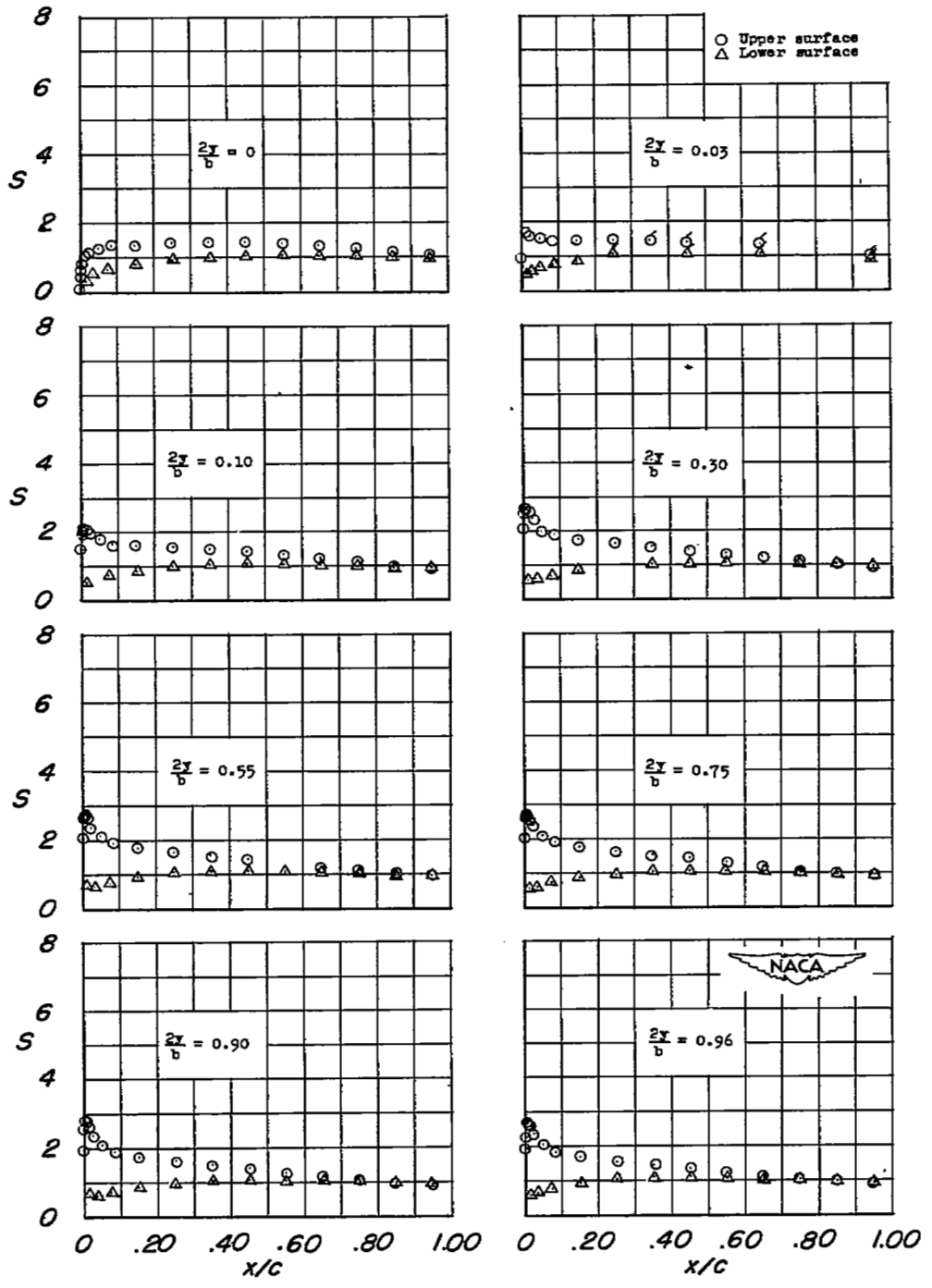

(f) $\alpha = 6.8^{\circ}$.

Figure 6.- Continued.

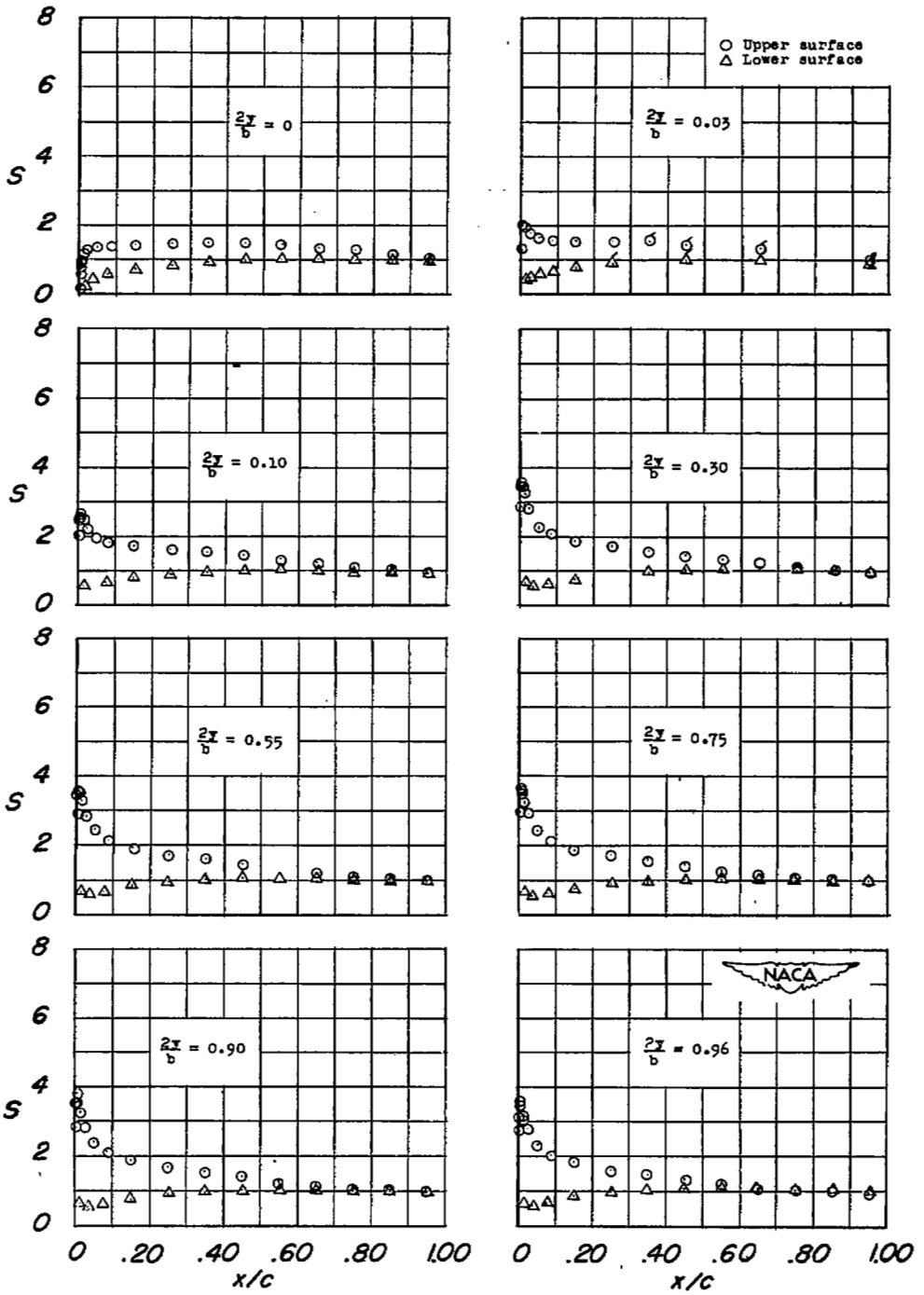

(g) $\alpha = 8.8^{\circ}$.

Figure 6.- Continued.

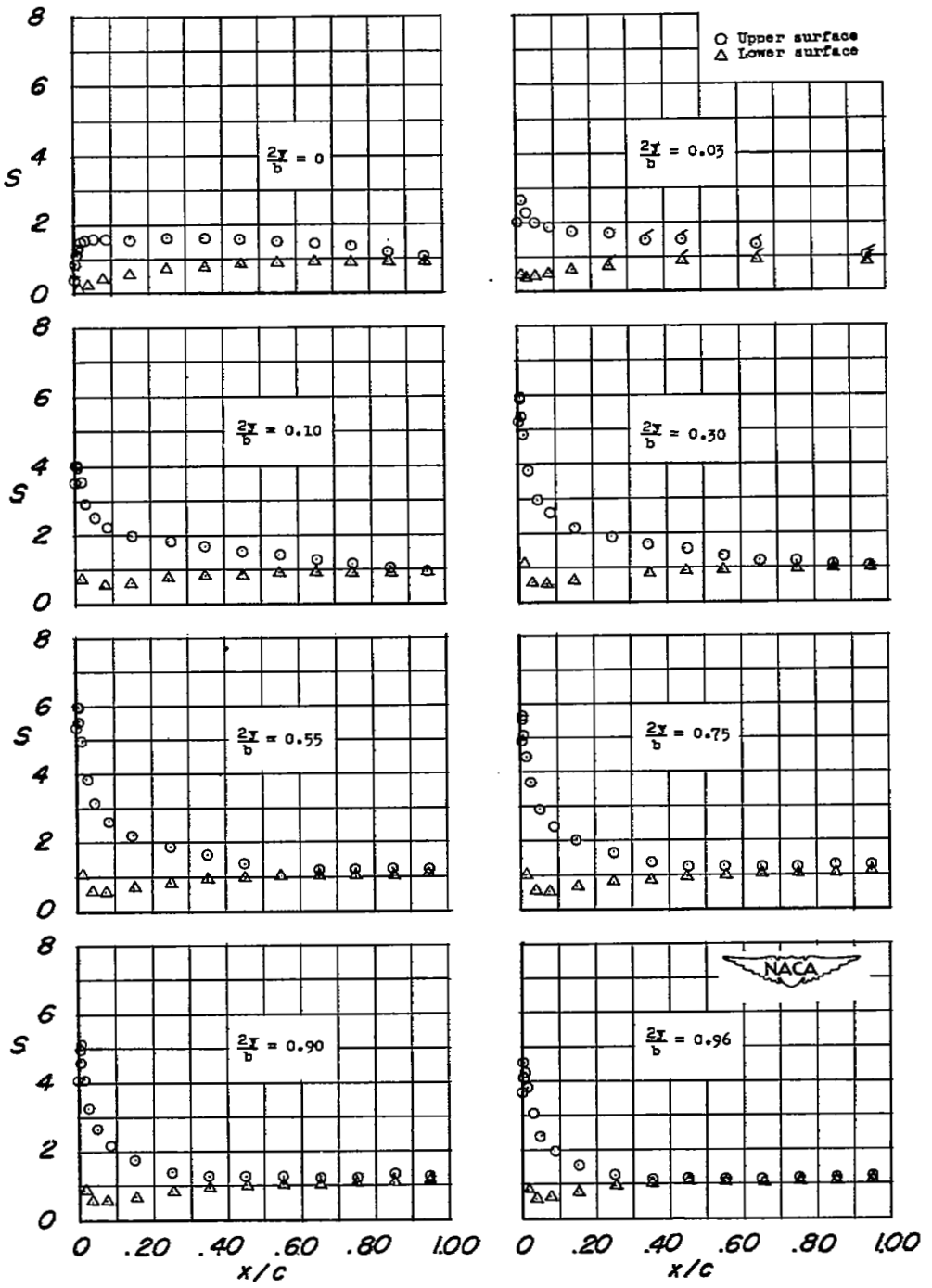

(h) $\alpha = 12.9^{\circ}$.

Figure 6.- Continued.

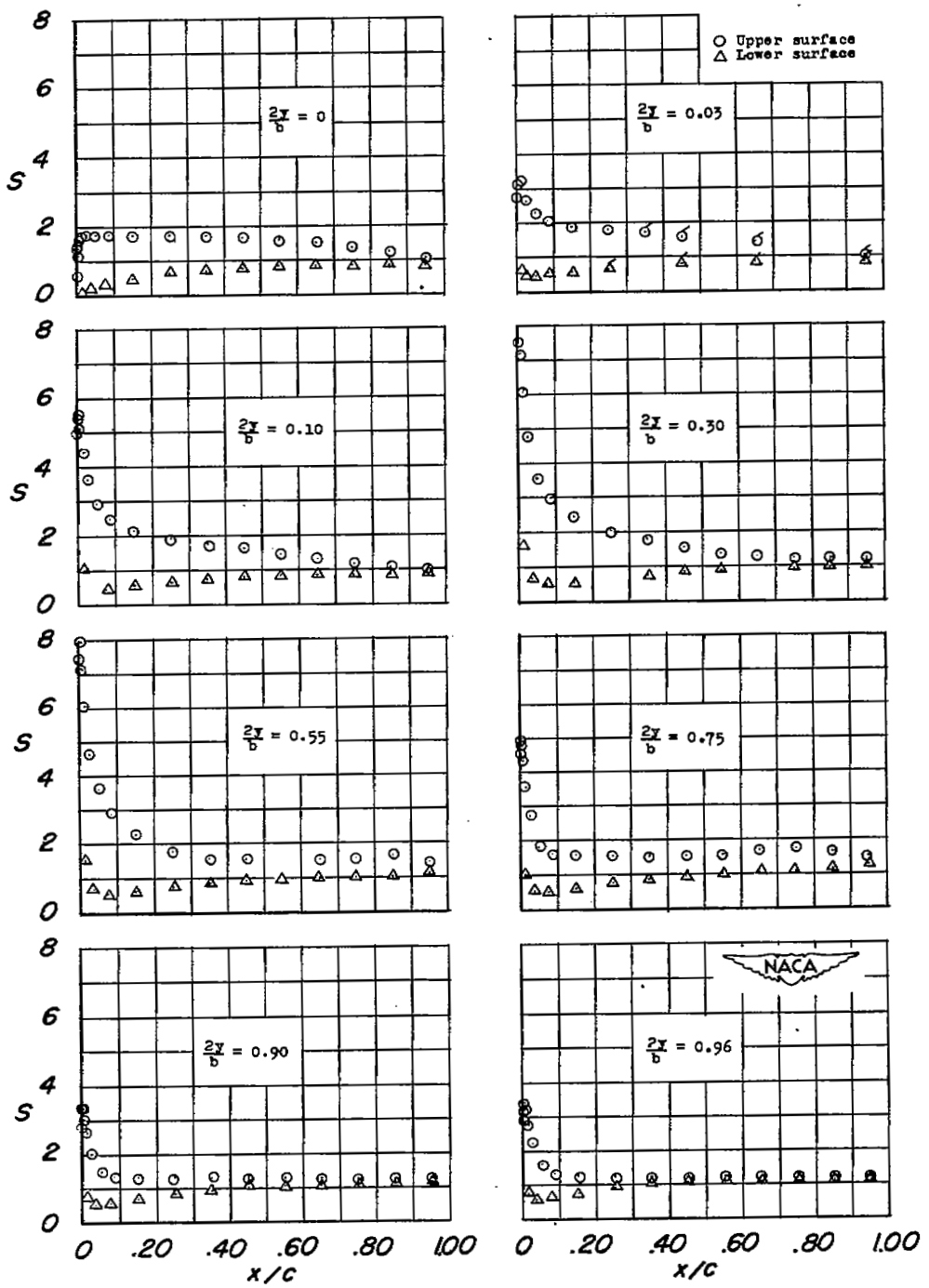

(i) $\alpha = 15.9^{\circ}$. (See table I for values of S at leading edge of stations 0.30b/2 and 0.55b/2.)

Figure 6.- Continued.

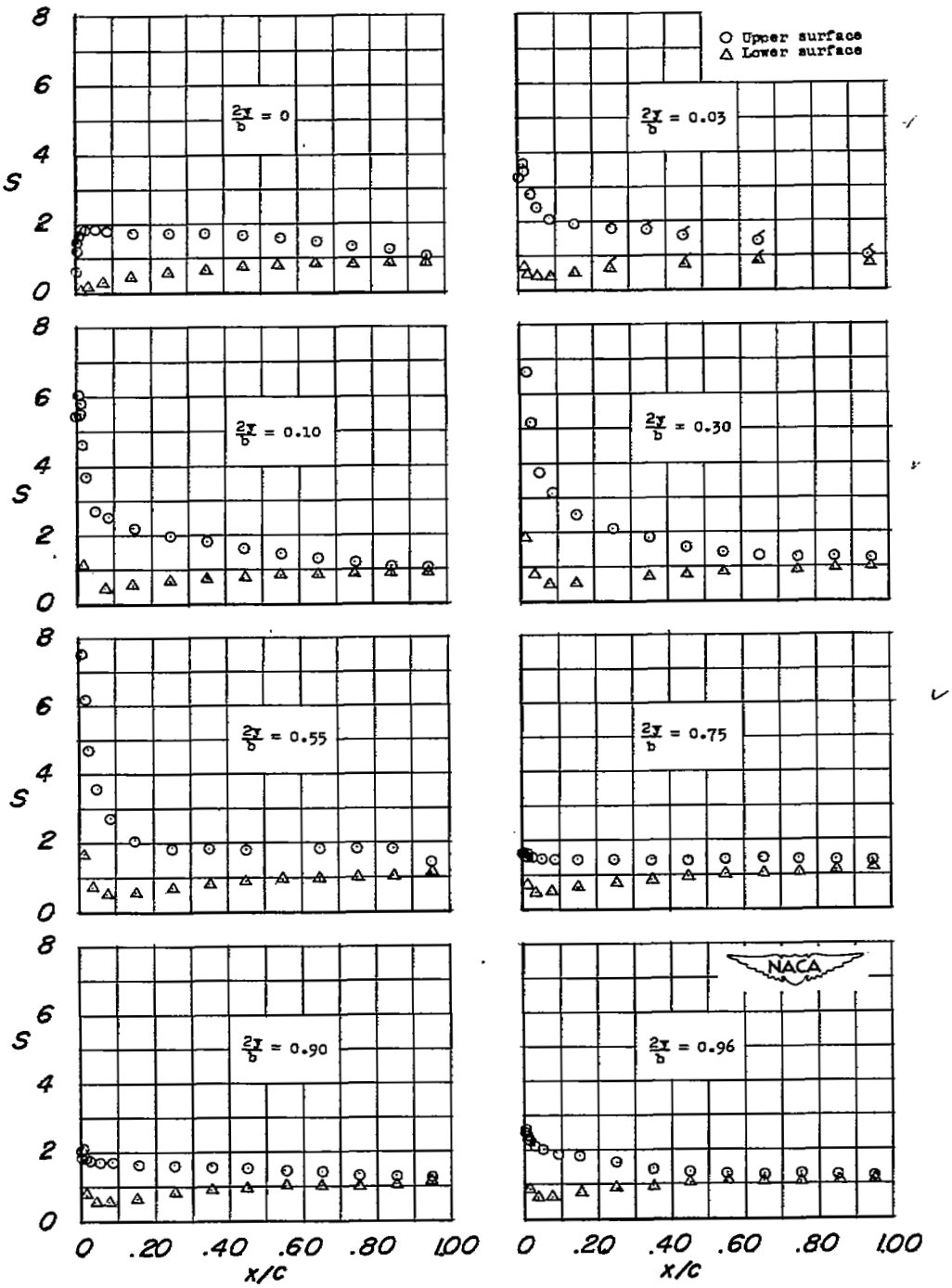

(j) $\alpha = 17.0^{\circ}$. (See table I for values of S at leading edge of stations 0.30b/2 and 0.55b/2.)

Figure 6.- Continued.

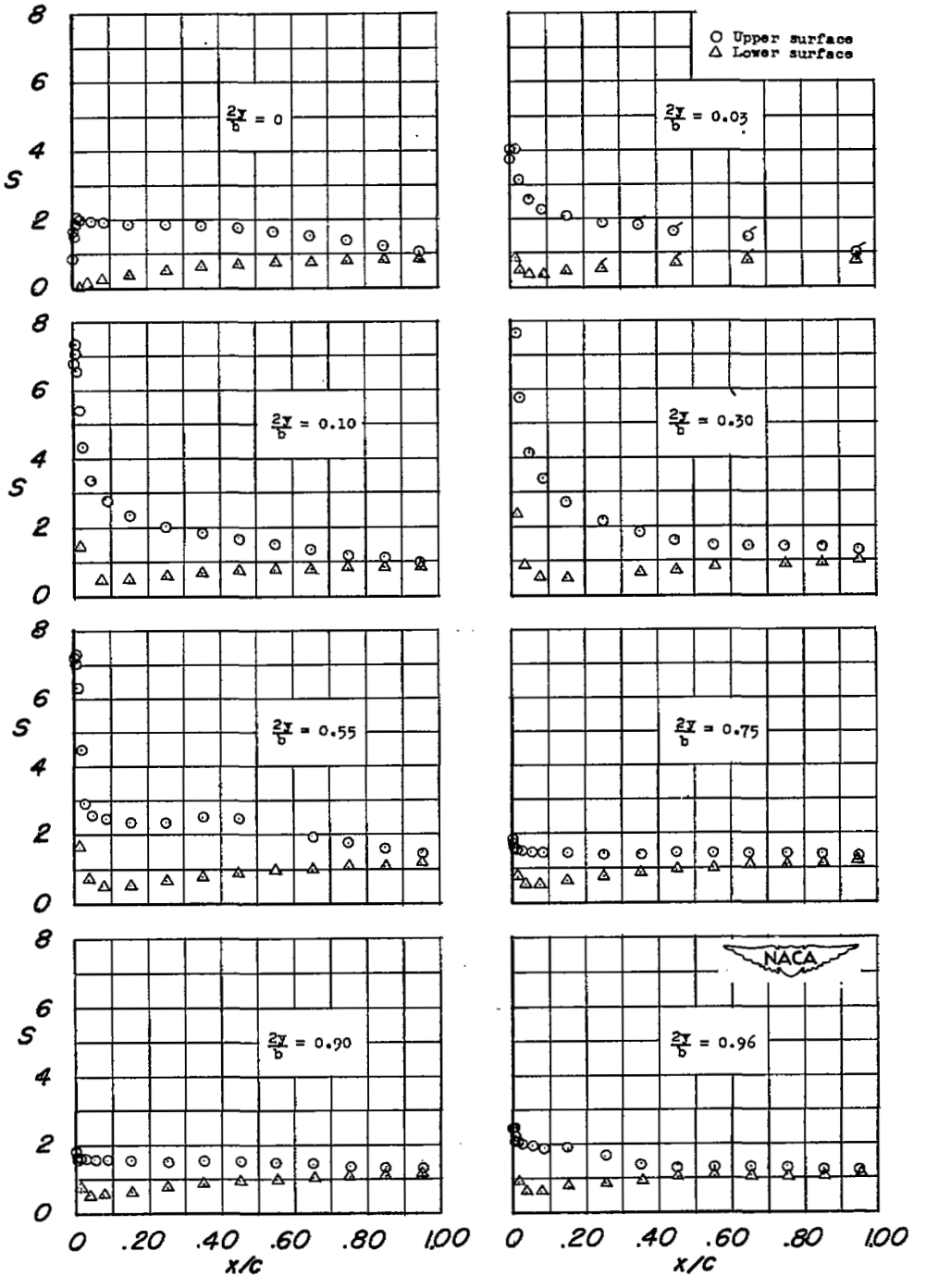

(k) $\alpha = 19.0^{\circ}$. (See table I for values of S at leading edge of station 0.30b/2.)

Figure 6.- Continued.

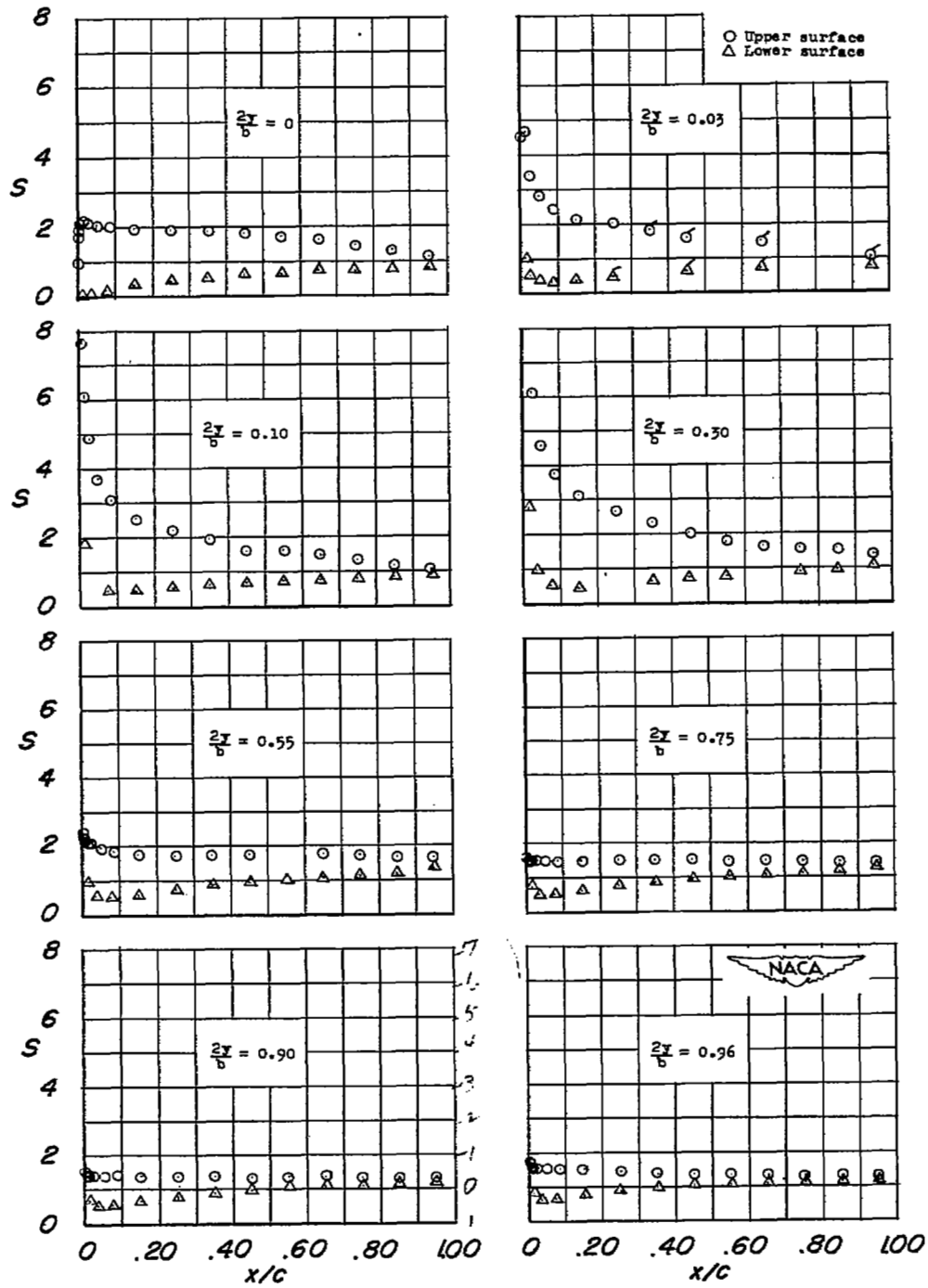

(l) $\alpha = 21.0^{\circ}$. (See table I for values of S at leading edge of stations 0.10b/2 and 0.30b/2.

Figure 6.- Continued.

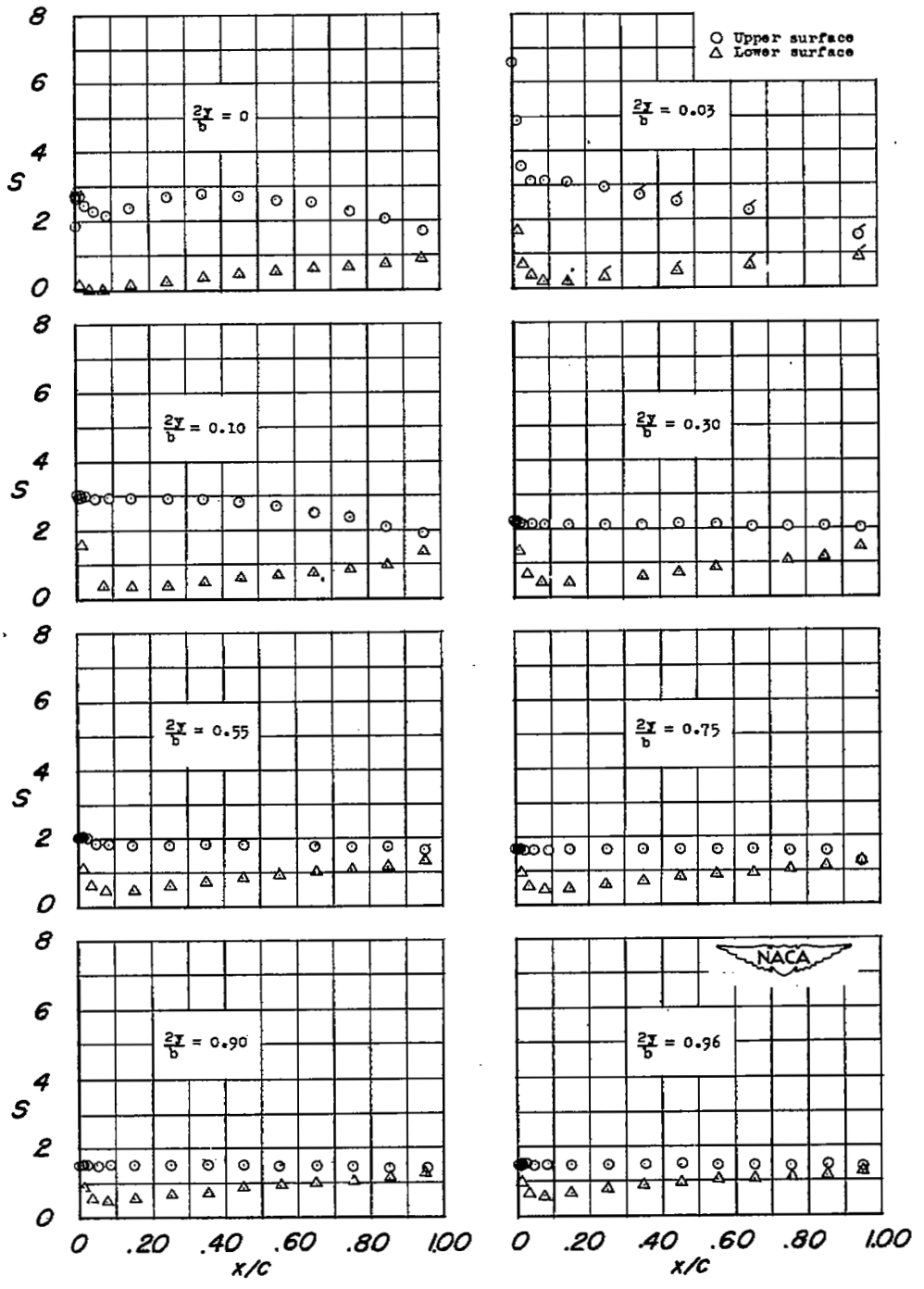

(m) $\alpha = 31.0^{\circ}$.

Figure 6.- Concluded.

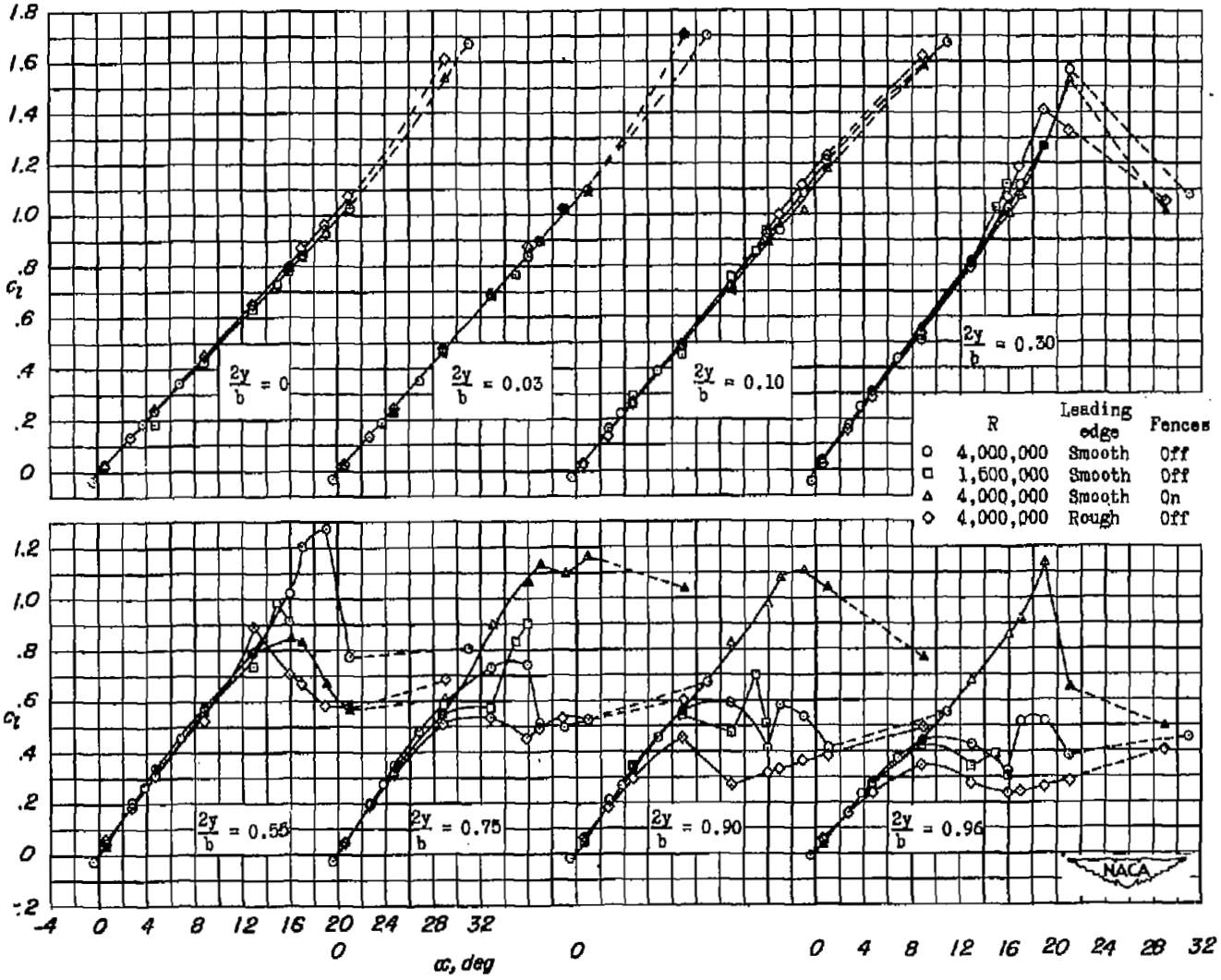

Figure 7.- Effects of Reynolds number variation, fences, and leading-edge roughness on the section lift characteristics.

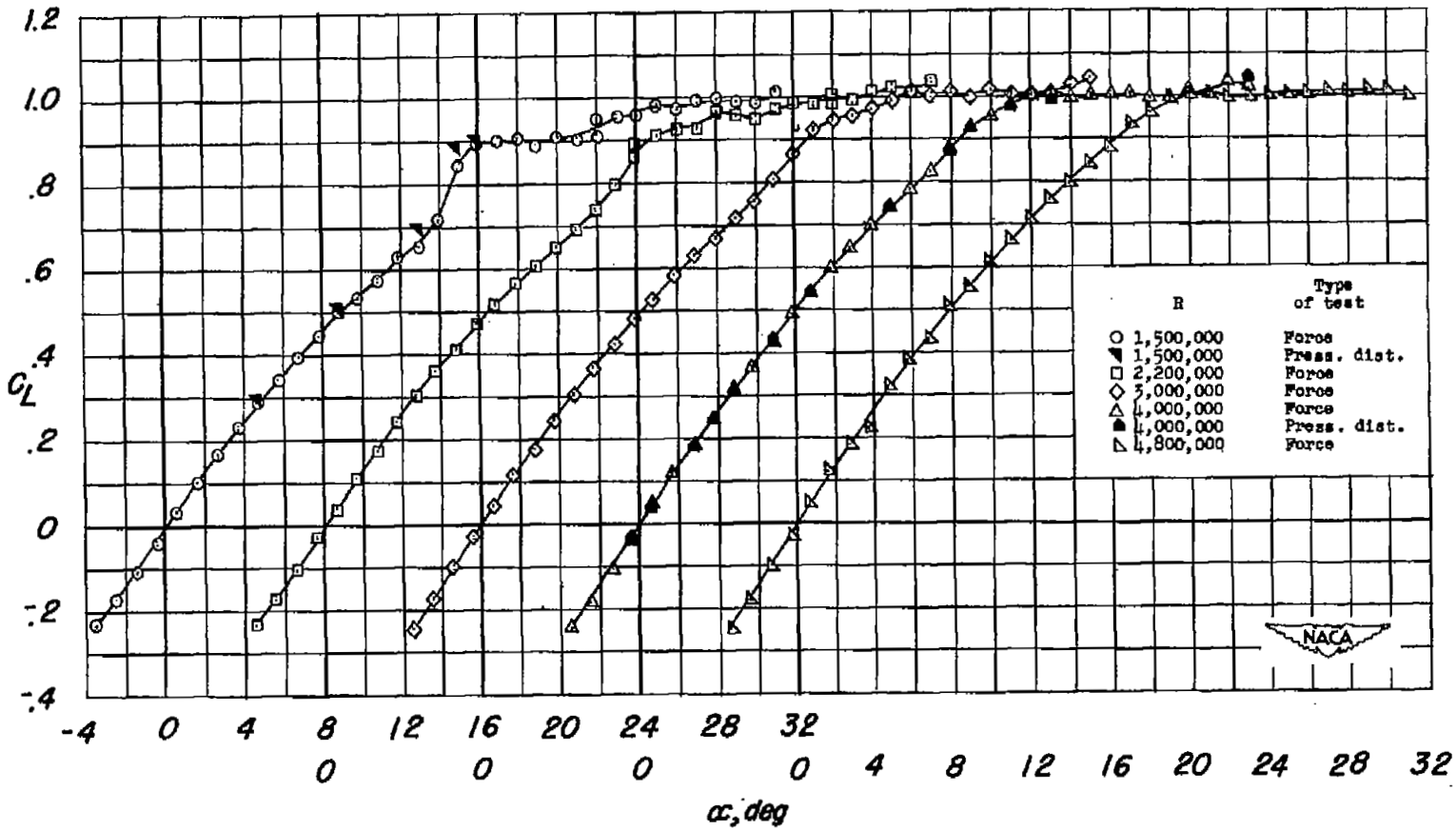

(a) Lift.

Figure 8.- Force and moment characteristics of the plain wing through a Reynolds number range.

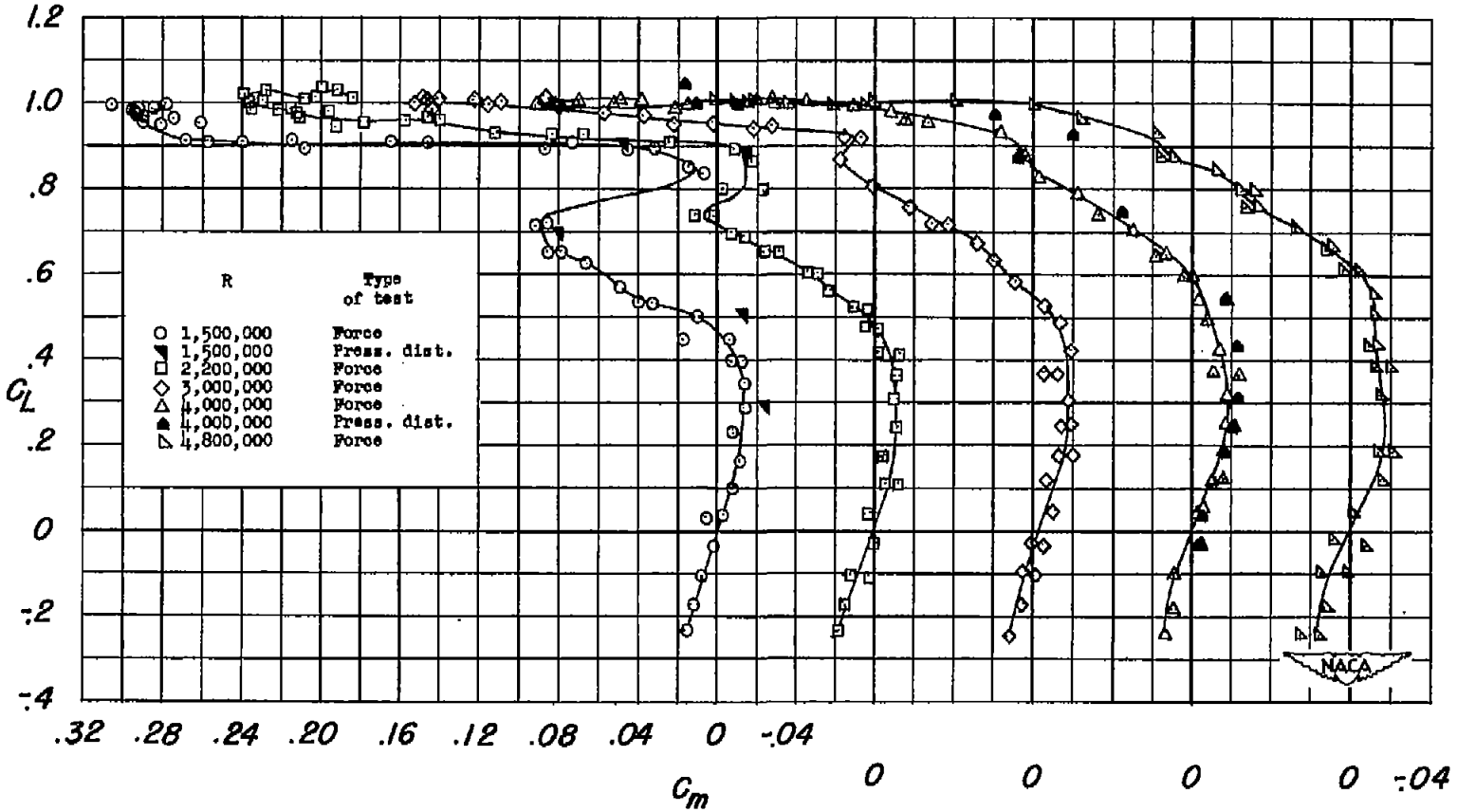

(b) Pitching moment.

Figure 8.- Continued.

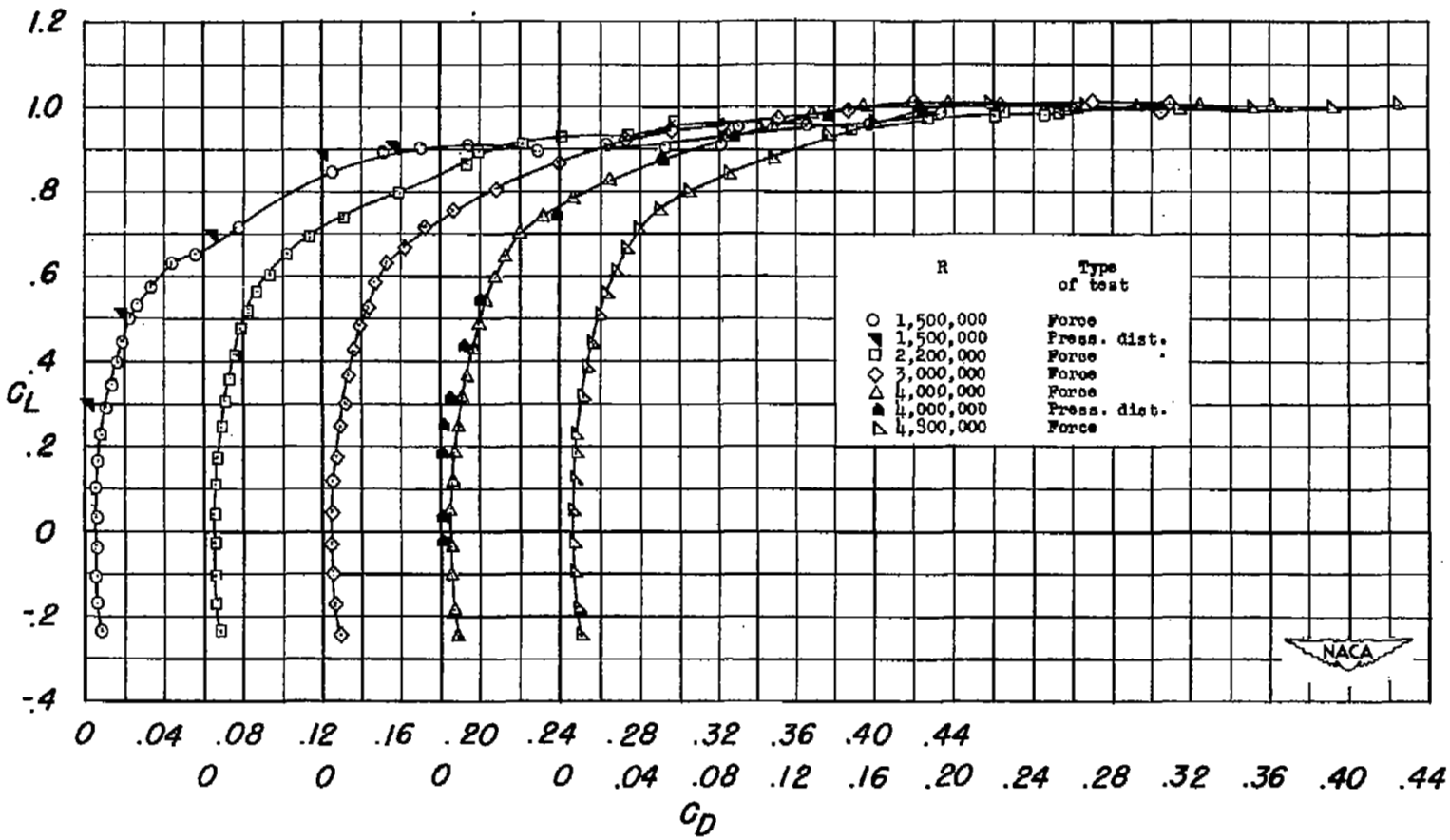

(c) Drag.

Figure 8.- Concluded.

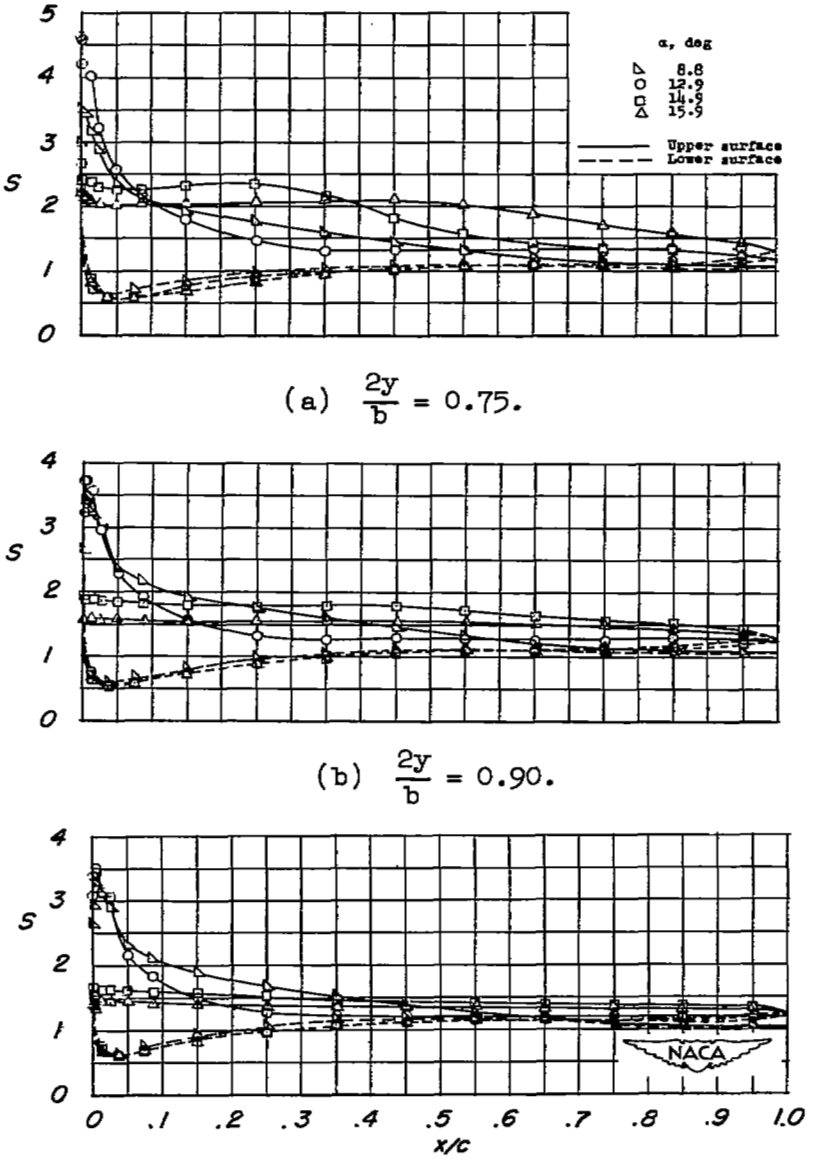

(a) $\frac{2y}{b} = 0.75$.

(b) $\frac{2y}{b} = 0.90$.

(c) $\frac{2y}{b} = 0.96$.

Figure 9.- Chordwise pressure diagrams for the plain wing. R = 1,500,000.

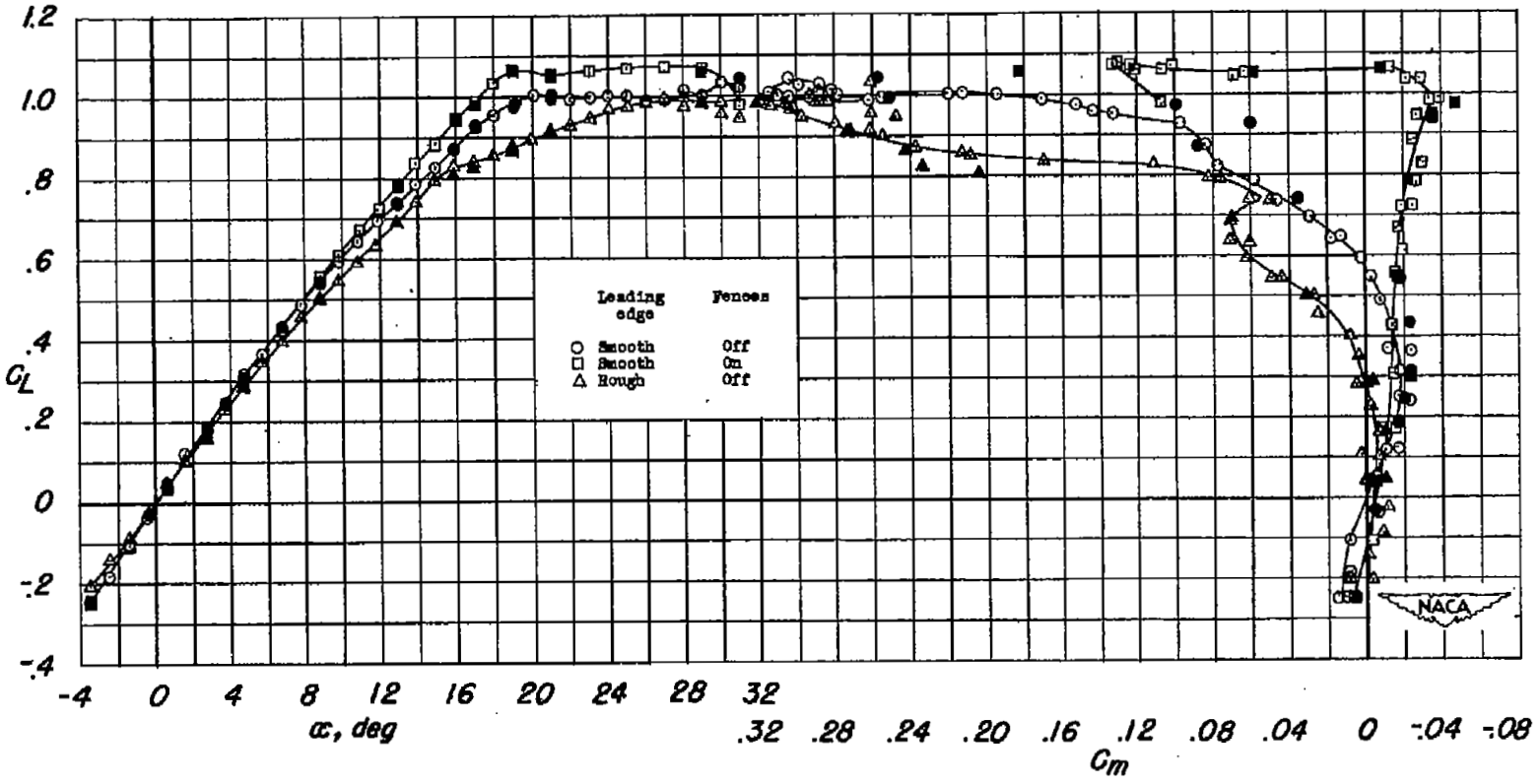

(a) Lift and pitching moment.

Figure 10.- Effects of chordwise fences and leading-edge roughness on the force and moment characteristics of the wing. R = 4,000,000. (Solid symbols indicate data from pressure-distribution tests.)

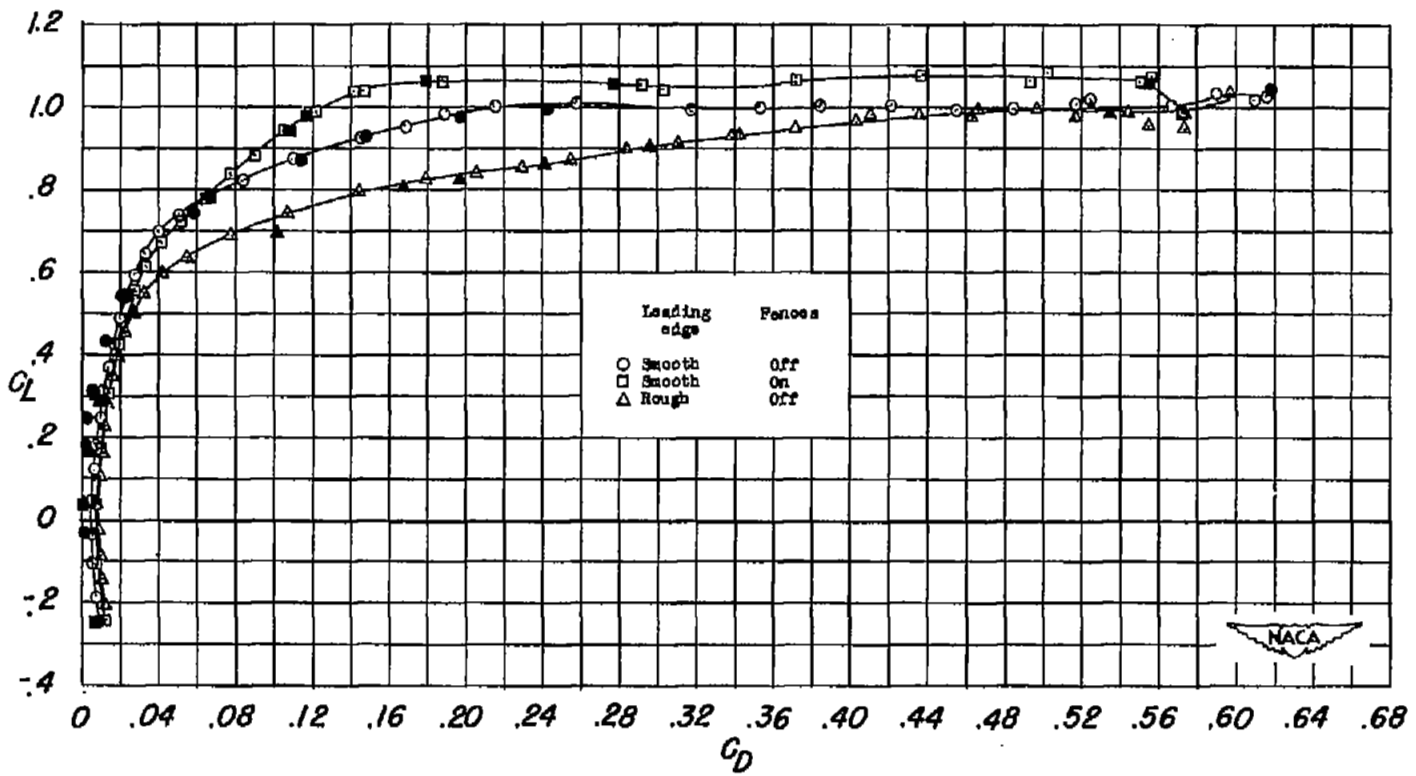

(b) Drag.

Figure 10.- Concluded.

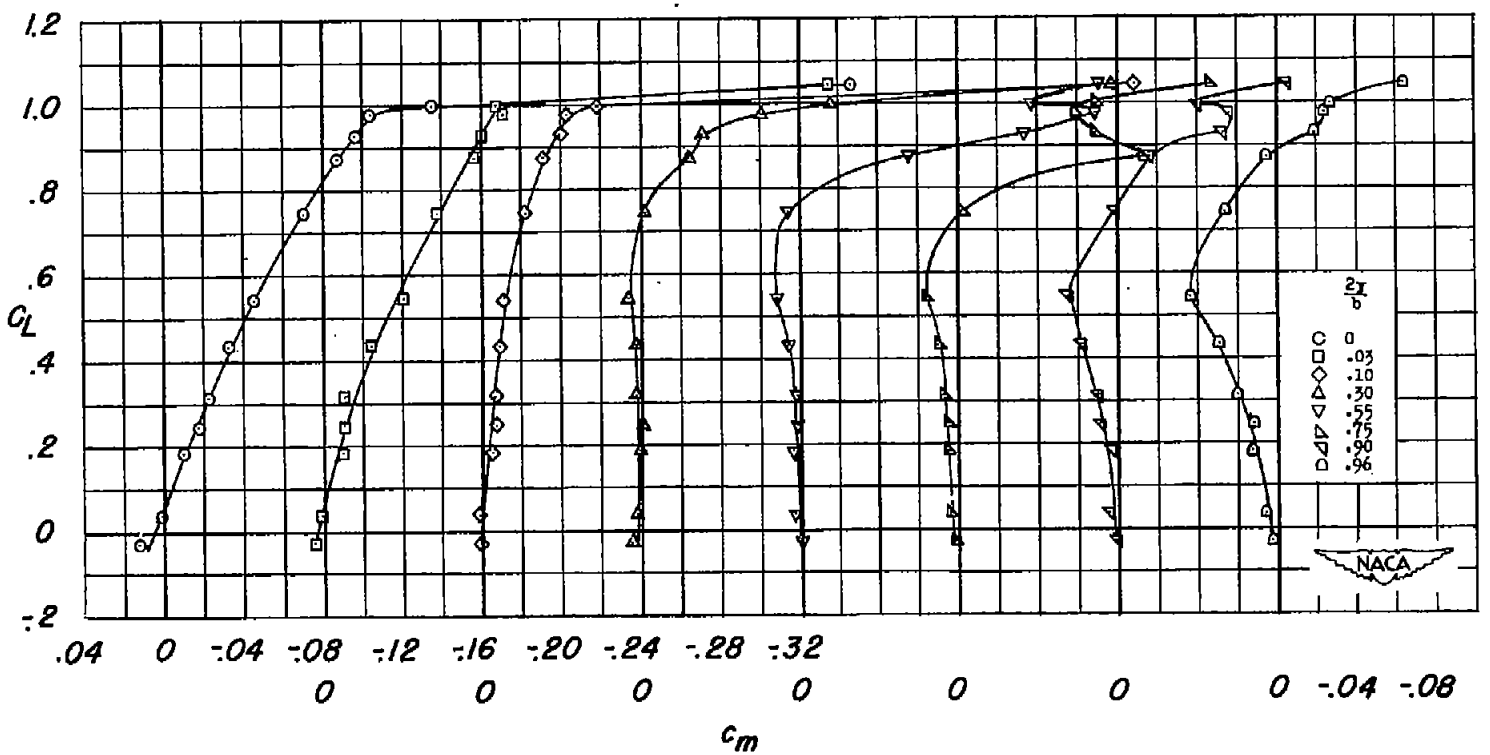

(a) Pitching moment.

Figure 11.- Section pitching-moment and drag characteristics of the plain wing. R = 4,000,000.

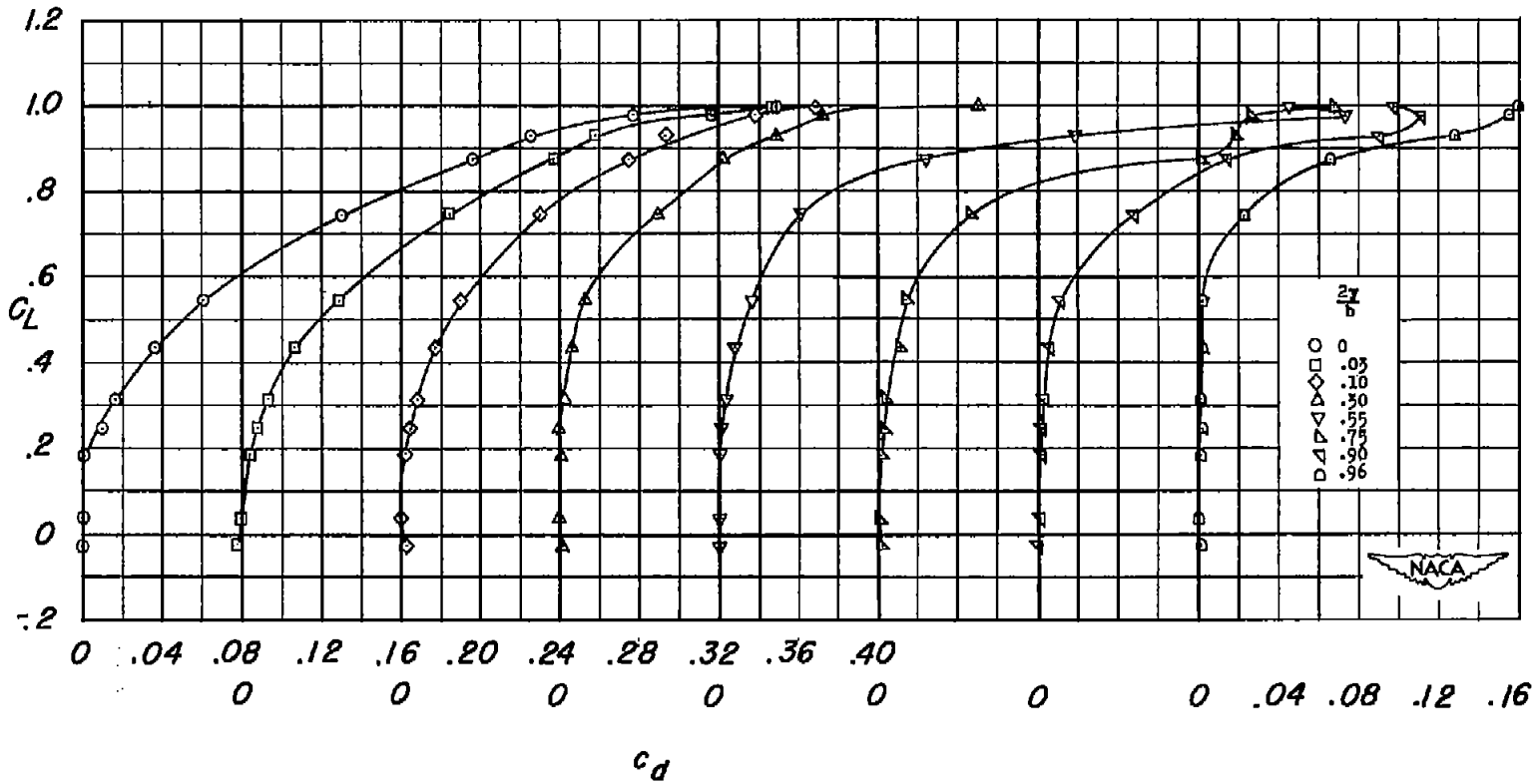

(b) Drag.

Figure 11.- Concluded.

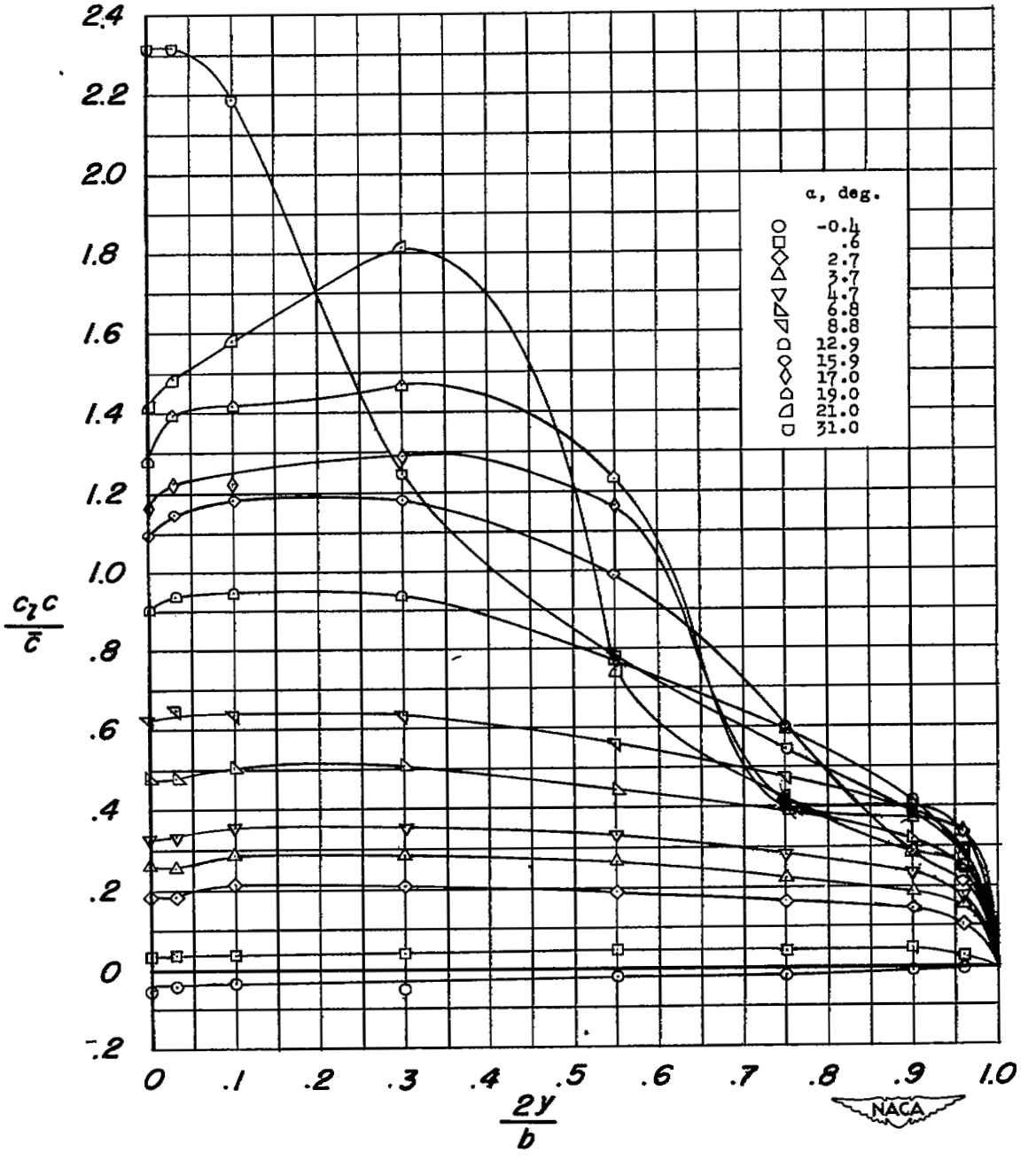

(a) Lift loading.

Figure 12.- Span loading characteristics of the plain wing. R = 4,000,000.

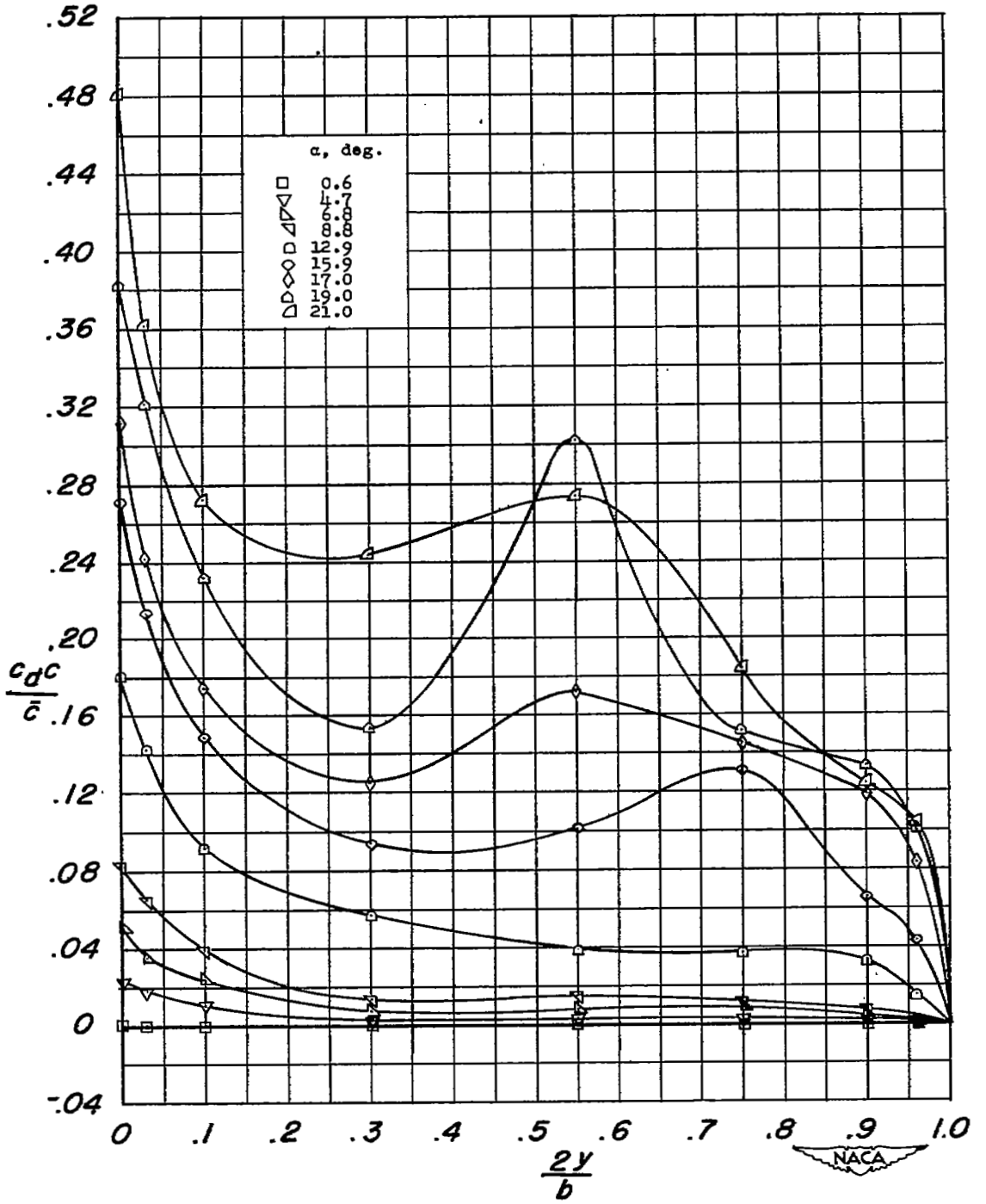

(b) Drag loading.

Figure 12.- Concluded.

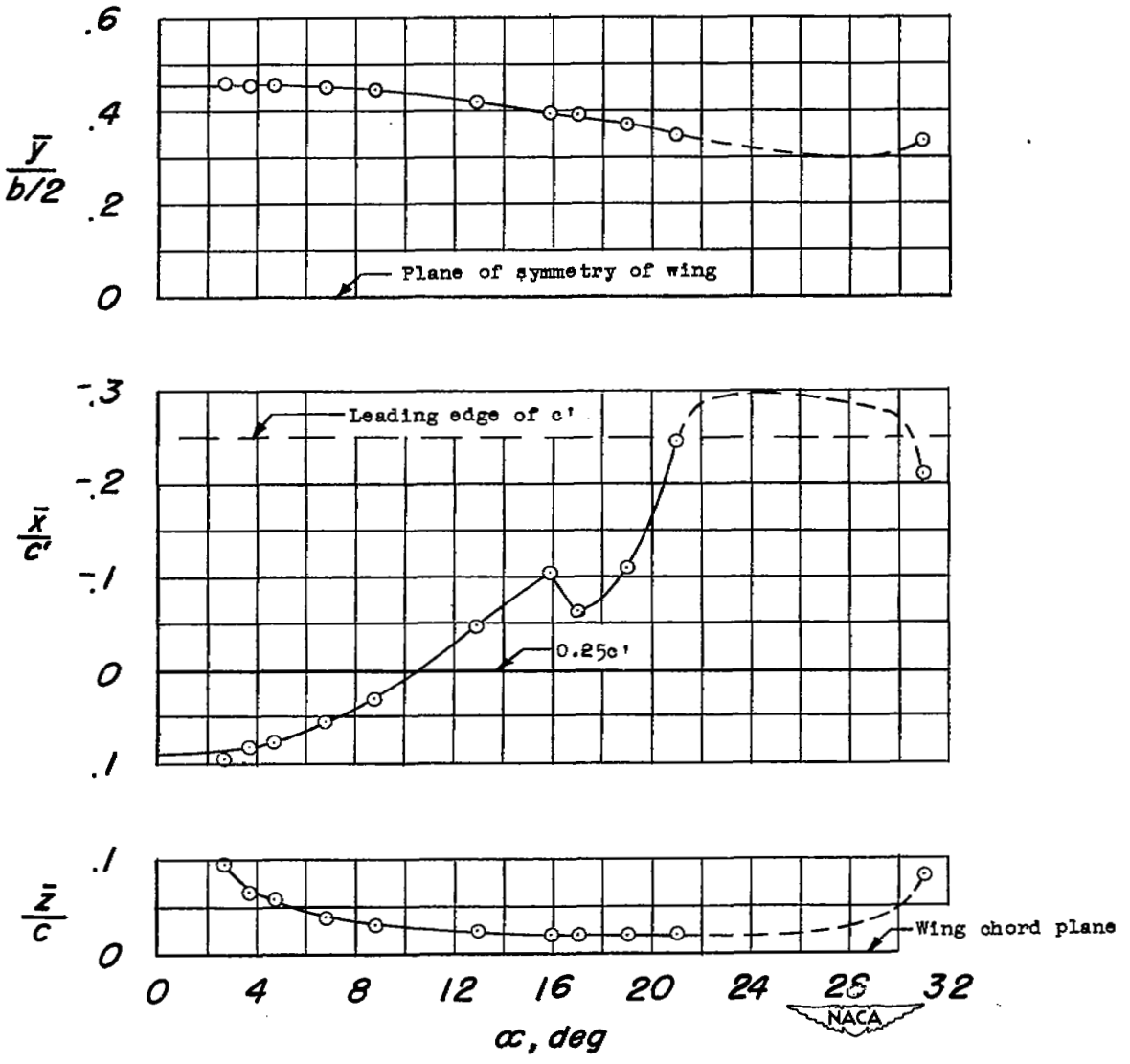

Figure 13.- Spanwise, chordwise, and vertical centers of pressure of the plain wing. R = 4,000,000.

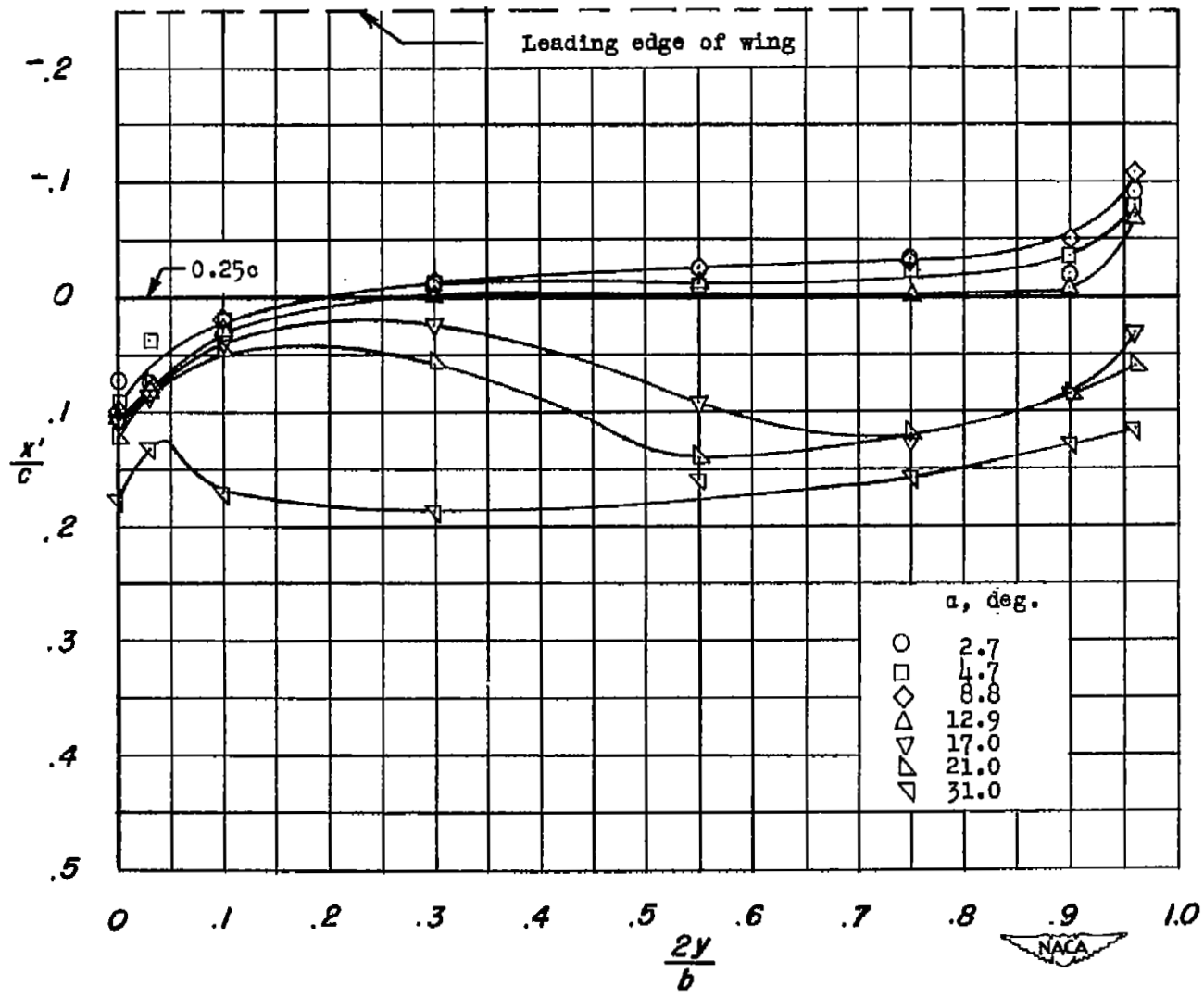

Figure 14.- Local chordwise centers of pressure for several angles of attack of the plain wing. R = 4,000,000.

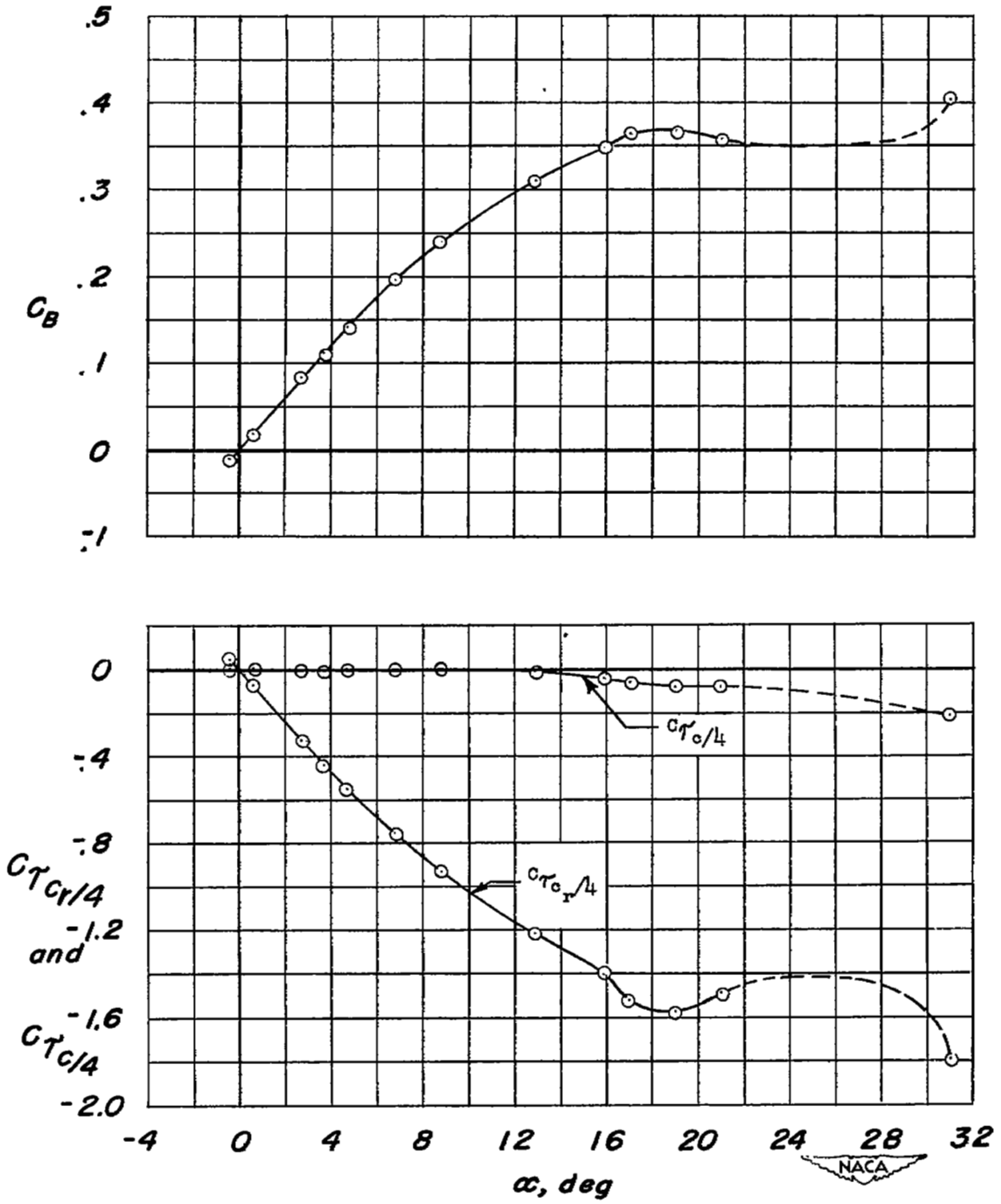

Figure 15.- Bending- and twisting-moment characteristics of the plain wing. R = 4,000,000.